Trinity College Dublin
Coláiste na Tríonóide, Baile Átha Cliath
The University of Dublin

Smurfit Institute of Genetics
Trinity College Dublin

Investigating the molecular mechanisms that control the transformation of leaves into floral organs

A thesis submitted in candidature for the degree of M.Sc.

Kate Horgan
Supervisor: Prof. Frank Wellmer
March 2021

Declaration:

I declare that this thesis has not been submitted as an exercise for a degree at this or any other university and it is entirely my own work.

I agree to deposit this thesis in the University's open access institutional repository or allow the library to do so on my behalf, subject to Irish Copyright Legislation and Trinity College Library conditions of use and acknowledgement.

Signed: Kate Horgan

Date: March 31st 2021

Summary of Work Undertaken:

Arabidopsis thaliana is the model plant which has been used to elucidate the molecular and genetic processes which underlie floral organogenesis. This is the process in which the four floral organs are formed which is mediated by four classes of master regulator transcription factors. Extensive research over the past three decades has illuminated how these factors control the formation of the floral organs, however the downstream processes of these master regulators is not well understood. This research aims to investigate the molecular mechanisms that control the transformation of leaves into the four floral organs. In particular, this research examines how the floral homeotic factor AGAMOUS regulates the genes involved in organ polarity specification.

Acknowledgements

List of Abbreviations

Term	Abbreviation
AGAMOUS	*AG*
Androgen Receptor	AR
APETALA1	*AP1*
APETALA2	*AP2*
APETALA3	*AP3*
ARABIDOPSIS HOMEOBOX-LEUCINE ZIPPER 4	ATH4
ARGONAUTE	*AGO*
Artificial microRNA	AmiRNA
ASYMMETRIC LEAVES1-2	*AS1-2*
AUXIN RESPONSE FACTOR2-4	*ARF2-4*
Base pair	bp
BR-ENHANCED EXPRESSION 1	*BEE1-3*
Cauliflower Mosaic Virus 35S promoter	35S
Chromatin Immunoprecipitation	ChIP
Clustered Regularly-Interspaced Short Palindromic Repeats	CRISPR
Columbia-0	Col-0
Complementary DNA	cDNA
CRABS CLAW	*CRC*
CUP-SHAPED COTYLEDON	*CUC*
Dexamethasone	DEX
DICER-LIKE1	*DCL1*
Differential Gene Expression	DEG
Dihydrotestosterone	*DHT*
DORNRÖSCHEN	*DRN*
DORNRÖSCHEN-LIKE	*DRNL*
Ethylene Response Factors	*ERF*
ETTIN	*ETT*
Floral Induction System	FIS
GLABRA1,3	*GL1*
Glucocorticoid Receptor	*GR*
Golden2, ARR-B and Psr1	*GARP*
HOMEOBOX-LEUCINE ZIPPER 3	*HAT3*

Homeodomain/leucine zipper	*HD-ZIP*
Inflorescence Meristem	IM
KANADI1-4	*KAN1-4*
KNUCKLES	*KNU*
Landsberg *erecta*	L-*er*
LATERAL ORGAN BOUNDARIES	*LOB*
LEAFY	*LFY*
MCM1-AGAMOUS-SRF-DEFICIENS	MADS
microRNA	miRNA
Next Generation Sequencing	NGS
No Reverse Transcriptase Control	*NRT*
No Template Control	*NCT*
NOZZLE	*NZZ*
Nucleotide	nt
PHABULOSA	*PHB*
PHAVOLUTA	*PHV*
PISTILLATA	*PI*
Polymerase Chain Reaction	PCR
Primary-miRNA	Pri-miRNA
Reverse Transcription Quantitative Polymerase Chain Reaction	RT-qPCR
REVOLUTA	*REV*
RNA induced silencing complex	*RISC*
RNA integrity number	*RIN*
RNA-sequencing	RNA-seq
Root Apical Meristem	RAM
SEPALLATA1-4	*SEP1-4*
Shoot Apical Meristem	SAM
SPOROCYTELESS	*SPL*
SUPERMAN	*SUP*
TARGET OF EAT1	*TOE1*
TRANSPARENT TESTA GLABRA 1	*TTG*
UBIQUITIN 10	*UB10*
WUSCHEL	*WUS*
YABBY	*YAB*

Table of Contents

Chapter 1. Introduction

Flowers contain the reproductive organs of angiosperms, or flowering plants. Because they are often aesthetically appealing and produce much of the food humans and their livestock consume, they have been of great interest to people for centuries, and biologist have extensively studied flowers to better understand their functions and to optimize crop yields. In recent decades, much has been learned about the genetic basis of flower development, and scientists have begun to explore the evolutionary history of flowers using molecular approaches. The latter work can be seen as a direct continuation of research that started several centuries ago. For example, in his ground-breaking book *On the Origin of Species by Means of Natural Selection, or the Preservation of Favoured Races in the Struggle for Life*, Charles Darwin describes that evolution happens in a slow, incremental manner rather than as a sudden burst of diversity (Darwin, 1859). However, Darwin was puzzled when he considered the evolution of angiosperms because many morphologically diverse species seemed to have suddenly appeared in the fossil record. Because this did not agree with the ideas he had outlined in the *Origin of Species*, he used phrases such as "an abominable mystery" and "a most perplexing phenomenon" to express his wonder about angiosperm evolution (Darwin, 1879).

Recent evidence from the fossil record has shown that the evolution of flowering plants may not have been quite as sudden as it appeared to Darwin in the 19th century. The earliest angiosperms in the fossil record are approximately 200 million years old, and within a relatively short evolutionary time period, they appeared in an astounding array of different shapes and sizes (Li *et al.*, 2019; Ramírez-Barahona, Sauquet and Magallón, 2020). This suggests that flowering plants had a massive leap in diversity shortly after they came into existence. It now appears that this rapid burst of diversity was driven mainly by plant-pollinator interactions as well as whole genome duplication events (Dilcher, 2000; Jiao *et al.*, 2011; Soltis *et al.* 2019). In fact, in our modern world, angiosperms represent 90% of all extant plant species with at least 260,000 species classified in 453 families (Soltis *et al.* 2019). This begs the questions, how did angiosperms come to be; what did the first flowers look like; and why did angiosperms become so spectacularly successful?

While the diversity and morphology of flowers greatly varies, their development follows a common blueprint. A key aspect of this common blueprint is the conversion of leaf-like

structures into floral organs. This concept was originally proposed by the poet, playwright, statesman and naturalist Johann Wolfgang von Goethe in 1790 in his seminal treatise *Versuch die Metamorphose der Pflanzen zu erklären* (von Goethe, 1790), a book that is known as *The Metamorphosis of Plants* in the English-speaking world. Genetic and molecular results supporting Goethe's conjecture have accumulated over the past 30 years and there is now ample evidence for a model (which will be discussed in detail in the following sections) where several classes of floral homeotic transcription factors work together in a combinatorial manner to modify the developmental programme for leaves to bring about the formation of different types of floral organs. While immense progress has been made in deciphering the molecular pathways involved in this process, how exactly the floral homeotic transcription factors mediate the transformation of leaf-like structures into floral organs is not well understood.

This introduction will provide an overview of the molecular basis of flower development with a focus on the model plant *Arabidopsis thaliana* (Arabidopsis, hereafter). It will also highlight our current understanding of the leaf-to-flower transformation with a particular focus on organ polarity, which was the focus of the work presented in this thesis.

1.1. The Fundamentals of Flower Development

Angiosperms follow a developmental progression from embryo to mature plant (Krizek and Fletcher, 2005). During embryogenesis, they develop two apical meristems, which contain undifferentiated stem cells: the root apical meristem (RAM), which accounts for the root system, and the shoot apical meristem (SAM) from which all above ground organs, such as leaves, shoots and flowers, are derived (Sharma, 2002; Jiang and Feldman, 2005). Both the SAM and RAM are indeterminate structures meaning that their growth cessation is not genetically pre-determined and that they can maintain a stem cell population, at least in principle, indefinitely (Carles and Fletcher, 2003; Krizek and Fletcher, 2005).

During the vegetive phase of development, the SAM produces leaf primordia on its flanks. Upon the transition to flowering, the shoot bolts and the SAM becomes the inflorescence meristem. In Arabidopsis, the inflorescence meristem produces initially a limited number of cauline leaves and axillary meristems, before it initiates floral meristems on its flanks in

specific positions, one floral meristem at a time (Fig. 1.1A) (Alvarez-Buylla *et al.*, 2010). Floral meristems are spherical mounds of undifferentiated cells that in Arabidopsis produce four different types floral organs: sepals, petals, stamens and carpels (Fig. 1.1B). These floral organs are arranged in four distinct concentric circles, or whorls. A typical Arabidopsis flower consists of four sepals in the outermost whorl, four petals in the second whorl, six stamens in the third whorl and two carpels in the innermost whorl that fuse to form a gynoecium (Smyth *et al.*, 1990). The initiation of organ primordia in the different whorls occurs sequentially from the outside of the flower to its centre, meaning that sepals are being initiated first and carpels last. In contrast to the apical meristems, floral meristems do not grow indefinitely. Their development ceases and their stem cells terminate after carpel primordia have been initiated. The termination of floral meristems must be precisely timed to ensure that flowers with a particular size and form are made (Krizek and Fletcher, 2005). This temporal control of floral meristem activity is mediated by a complex network of interacting regulatory genes (as summarized in: Denay *et al.*, 2017; Xu *et al.*, 2019; and Chang *et al.*, 2020).

The formation of flowers is a vital step in angiosperm development. Maximal reproductive success depends on the timing of flowering in order to balance the number of seeds produced with resources available. In order to produce flowers, the plant must undergo a transition from vegetative to reproductive growth. This transition is governed by environmental and endogenous signals, which include day length, ambient temperature and prolonged exposure to cold (vernalization), as well as metabolic and other endogenous signals such as developmental age (reviewed in: Srikanth and Schmid, 2011; Kinoshita and Richter, 2020). These signals are perceived by different receptors that activate distinct signal transduction pathways, which all converge on a small number of so-called floral pathway integrator genes, including *FLOWERING LOCUS T* and *SUPPRESSOR OF OVEREXPRESSION OF CONSTANS 1*. The floral pathway integrators then activate floral meristem identity genes such as *LEAFY (LFY)* and *APETALA1 (AP1)* to produce floral meristems on the flanks of the inflorescence meristem (Liu, Thong and Yu, 2009; Wagner, 2017). These floral meristem identity genes, which all code for transcription factors, ensure that primordia initiated along the periphery of the inflorescence meristem adopt a flower fate. They are also responsible for activating floral organ identity genes, which specify the different types of floral organs (reviewed in Thomson and Wellmer, 2019).
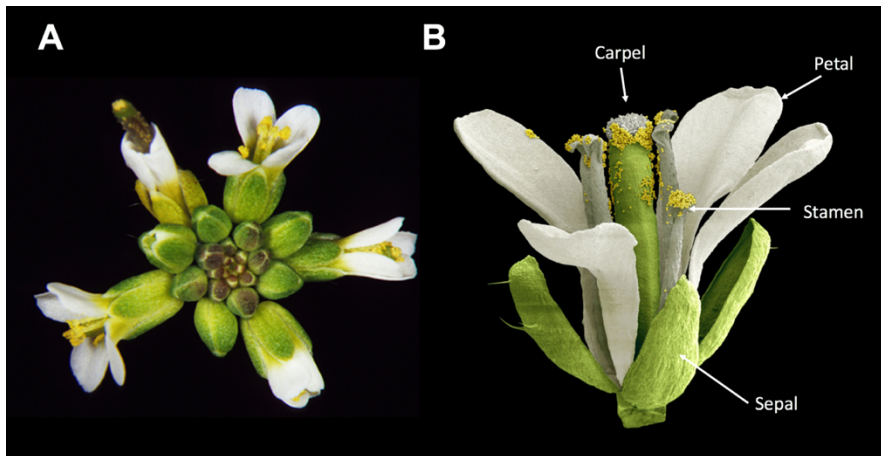
Figure 1.1: Structure of Arabidopsis flowers and inflorescences.

(A) An inflorescence of accession *Landsberg erecta*. Flowers are formed in a spiral, sequential manner with the oldest flowers on the outer edge and the youngest flowers at the centre of the inflorescence. **(B)** An Arabidopsis flower with the floral organs labelled - first whorl sepals, second whorl petals, third whorl stamens and fourth whorl carpels (which fuse to form the gynoecium). Images by José Luis Riechmann and Jürgen Berger, respectively.

1.2. Models of Flower Development

The floral organ identity genes were identified through mutants that are characterised by homeotic transformations, i.e. the replacement of one (or more) organ types by another (Fig. 1.2). For example, the *agamous* (*ag*) mutant lacks all reproductive organs (i.e., stamens and carpels) but has extra whorls of sepals and petals. Although such floral mutants were discovered in many angiosperm species, the genetic and molecular analysis of the affected genes was done primarily in Arabidopsis and *Antirrhinum majus* (snapdragon) (Bowman, 1989; Bowman, Smyth and Meyerowitz, 2012; Irish, 2017). A careful examination of the phenotypes of these mutants revealed similarities between some of them, leading to the floral homeotic mutants being divided into three distinct groups named A, B and C.

Further analysis of the phenotypes of double and triple mutant combinations revealed strong interactions between the affected genes. These results led to the realization that the mutated genes act in a combinatorial manner to specify the identities of the different types of floral

organs. This discovery led to the formulation of the ABC model (Schwarz-Sommer *et al.*, 1990; Coen and Meyerowitz, 1991), which has guided research in the field of flower development over the past 30 years. Because of its relative simplicity, it has arguably become one of the best known models in all of developmental biology. The model posits that class A genes specify sepals in the 1st floral whorl, while class A and B genes act together to form petals in the 2nd whorl. Class B and C genes specify stamens in the 3rd whorl and class C genes specify carpels in the 4th whorl in the centre of the flower. An important additional feature of the model is the assumption that A and C class genes act in a mutually antagonistic manner and prevent each other from being active in regions of the flower where the other gene activity is normally observed. In other words, A class genes would act to prevent C class genes from being active in the 1st and 2nd whorls, while C class genes would prevent A class genes from being active in the centre of the flower, i.e., in the 3rd and 4th whorls (Fig. 1.3 (1)) (Coen and Meyerowitz 1991).
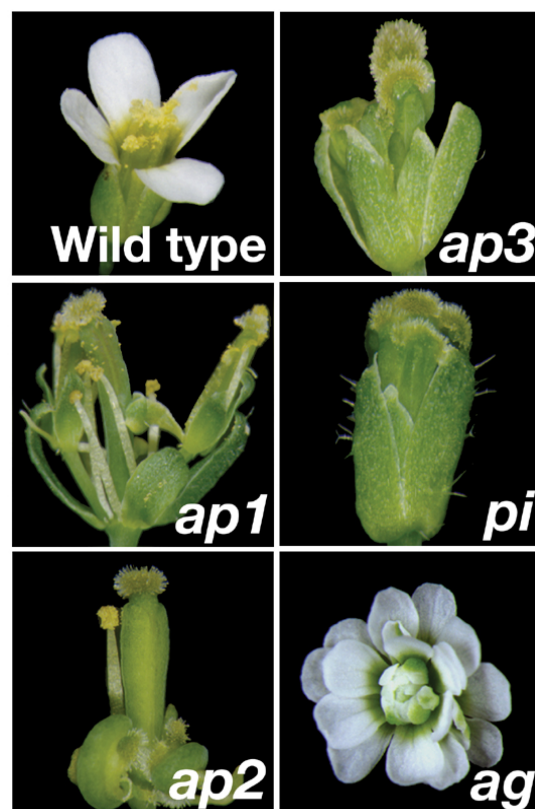
Figure 1.2: Floral homeotic mutants in Arabidopsis.

A wild-type flower and flowers of *ap1*, *ap2*, *ap3*, *pi* and *ag* mutants are shown. Figure modified from Wellmer *et al.*, 2004.

In Arabidopsis, five floral homeotic mutants were initially described and the affected genes were named based on the phenotypic defects of the mutants (Fig. 1.2). These include the above-mentioned *AP1* gene, which also acts as a floral meristem identity gene. Two other genes, *APETALA2* (*AP2*) and *APETALA3* (*AP3*), were named based on the phenotype that all three *apetala* mutants have in common, namely the absence of petals (although strong *ap1* mutants do occasionally form some petals (Irish and Sussex, 1990; Mandel *et al.*, 1992)). A fourth gene was named *PISTILLATA* (*PI*) because it forms extra pistils (this mutant is however largely indistinguishable from the *ap3* mutant and thus could have also been named '*ap4*' or similar). The fifth and final gene in the set of floral organ identity genes is the above-mentioned *AG*, which received its name from the fact that *ag* mutants do not form any gametes due to the complete absence of reproductive floral organs. Based on the phenotypes of the floral homeotic mutants, the floral organ identity genes were assigned to different classes as follows: A class: *AP1* and *AP2*; B class: *AP3* and *PI*; and C class: *AG*. The molecular cloning of these genes revealed that they all belong to the family of MADS (for MCM1, AGAMOUS, DEFICIENS, and Serum response factor) domain transcription factors, which is significantly enlarged in plants relative to other eukaryotes (Yanofsky *et al.*, 1990; Goto *et al.*, 1994; Jack, Fox and Meyerowltx, 1994; Jofuku *et al.*, 1994; Pařenicová *et al.*, 2003; Kaufmann, Melzer and Theißen, 2005). The only exception is *AP2*, which encodes the founding member of a large family of plant-specific transcription factors, the AP2/Ethylene Response Factors (ERF) (Okamuro *et al.*, 1997). The floral organ identity genes are generally expressed in the organs they are specifying (Yanofsky *et al.*, 1990; Goto *et al.*, 1994; Okamuro *et al.*, 1997). The regulatory mechanisms that ensure the expression of these genes in specific but overlapping domains is complex and has been extensively studied. As mentioned above, the floral meristem identity genes such as *LFY* play a key role in the onset of the expression of the floral organ identity genes, but additional inputs are required to ensure the restriction of expression to specific domains. These mechanisms rely on a multitude of additional transcriptional regulators, chromatin remodellers and microRNAs (Ó'Maoiléidigh, Graciet and Wellmer, 2014; Guo *et al.*, 2015; Chen *et al.*, 2018; Thomson and Wellmer, 2019; Xu *et al.*, 2019; Waheed and Zeng, 2020).

When double mutants between genes assigned to two different classes were generated, the resulting phenotypic abnormalities were largely in agreement with the predictions of the

ABC model. However, the model did not predict what would happen if all three gene activities, i.e. A, B , and C, would be inactivated simultaneously. Strikingly, it was found that in such triple mutants, floral organs were replaced with leaf-like structures (Bowman et al., 1991). This suggested not only that Goethe's hypothesis on the origin of floral organs was correct, but also that the floral organ identity genes are necessary for the transformation process. To test whether these genes were also sufficient to convert leaves into floral organs, they were ectopically expressed in plants. In these experiments, no transformation of leaves into floral organs was observed although in some cases leaf development was affected to some extent (Krizek and Meyerowitz, 1996; Mizukami and Ma, 1992). These results suggested that either the floral organ identity genes are insufficient for carrying out the transformation process (and thus are not true master regulators of floral organ specification) or that additional gene activities are needed for their functions.

A reverse genetics analysis of genes encoding additional MADS domain proteins then showed that four *SEPALLATA* genes *(SEP1-4)* encode partially redundant co-factors of the floral organ identity factors. These genes were named based on the phenotype of *sep1 sep2 sep3* triple mutant flowers, which show a conversion of all floral organs into sepals (Pelaz et al., 2000). The discovery of a fourth *SEP* gene (*SEP4*) and the analysis of a *sep* quadruple mutant showed a conversion of all four floral organ types into leaf-like structures with carpelloid features, thus overall resembling ABC triple mutants. To demonstrate that the ABC class transcription factors, together with the SEP co-factors, are sufficient to convert leaves in floral organs, different combinations of the transcription factors were ectopically expressed (Honma and Goto, 2001). For example, over-expression of *SEP3,* together with A and B class genes led to the conversion of leaves into petals (Honma and Goto, 2001). Furthermore these experiments showed that SEPs are needed in conjunction with B and C genes for the proper formation of floral organs and to impose floral determinacy (Pelaz et al., 2000; Ditta et al., 2004). Because genes that specify ovule development had been previously named 'D class genes' (Colombo *et al.*, 1995), the SEP transcription factors were added to the ABC model as the E class resulting in an "ABCDE" model for the specification of the different parts of the flower (Fig. 1.3 (2)).

As mentioned above, most of the genes involved in floral organ identity specification encode MADS-domain proteins (Kaufmann, Melzer and Theißen, 2005). These transcription factors have four structural domains that allow them to bind DNA as dimers and act as tetrameric

complexes that regulate the transcription of target genes (Fig. 1.3) (Theißen, Melzer and Rümpler, 2016). It has been proposed that these floral quartets interact with chromatin by binding to two so-called CArG-box motifs (5'-GG[A/T]$_6$CC-3') in the promoters of their target genes (Theißen, Melzer and Rümpler, 2016). This dual binding event likely leads, at least in some cases where there is some distance between the CArG-boxes, to looping of the DNA. From this, the so-called 'floral quartet model' was established to explain how the ABCDE classes of transcription factors interact to control the development of the different types of floral organs (Theißen and Saedler, 2001; Theißen, Melzer and Rümpler, 2016).

As mentioned above, one central aspect of the original ABC model is that A and C function genes work in a mutually antagonistic manner whereby the A class genes prevent the expression of the C class genes in the first two whorls and *vice versa* (Bowman, Smyth and Meyerowitz, 1991). Experimentally, it was shown that AP2 suppresses *AG* in the outer two floral whorls, however, AG does not control *AP2* expression levels. This was made clear as *AP2* transcripts do not accumulate in the third and fourth whorl of *ag* mutant flowers (Wollmann *et al.*, 2010). Instead, *AP2* transcripts are prevented from accumulating in the third and fourth whorls through the activity of members of the microRNA172 family of microRNAs (Wollmann *et al.*, 2010). It was further shown that members of the transcriptional co-repressor family TOPLESS/TOPLESS RELATED (TPL/TPR*)* and the HISTONE DEACTYLASE 19 (HDA19) are also required to suppress *AG* expression in outer floral whorls (Krogan, Hogan and Long, 2012). Chromatin Immunoprecipitation (ChIP) experiments demonstrated that a complex of AP2-TPL-HDA19 binds to regulatory regions of *AP3* and *SEP3*. Additionally, the expression of *AP3, PI* and *SEP3* was detected in the third and fourth whorl of plants lacking functional copies of *AP2, TPL* or *HDA19* (Krogan, Hogan and Long, 2012). Together, this data shows that AP2-containing complexes act as spatial regulators of gene expression during floral patterning.

Several caveats or limitations to the ABCDE model have been found (Fig 1.3 (2)). Firstly, true A function mutants have only been identified in Arabidopsis and a few other species. As both A and E function genes have been found to also specify the floral meristem at the very beginning of flower development, it was proposed that their combined activities, termed '(A)', lead to the ground state of a floral organ which is the sepal (Causier, Schwarz-Sommer and Davies, 2010). This led to the proposal of the (A)BCD model (Fig. 1.3 (3)). The model was further reduced to an (A)B(C) model (Causier, Schwarz-Sommer and Davies, 2010) as

C and D function genes are believed to have arisen from a sub-functionalisation event of an ancestral gene that carried both functions of C and D function genes in Arabidopsis. Evidence supporting this model stems e.g. from Petunia (*Petunia hybrida*) where C and D clade genes largely overlap (Heijmans *et al.*, 2012). This means that the model of flower development has developed from a simple ABC model to a more generalized (A)B(C) model over the span of almost three decades (Fig. 1.3 (4)).
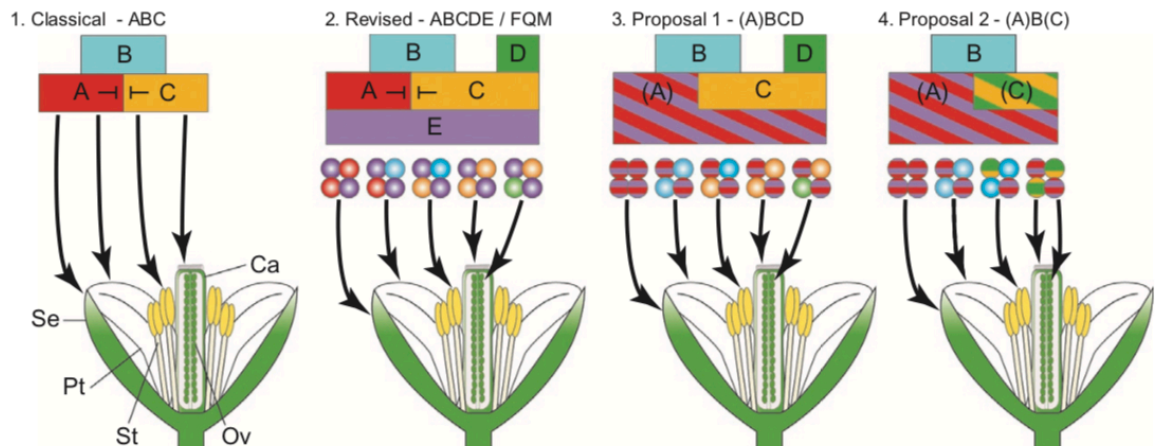
Figure 1.3: Proposed models for floral organ identity specification in Arabidopsis.

The floral homeotic genes act in a combinatorial manner to specify the different types of floral organs. Several models have been proposed for how floral organs are formed. See Section 1.2. for details of the models. The arrows specify the floral organs where the genes are active while the colours of the tetrameric complexes represent the class of gene. Classes of genes in brackets, e.g. (A), represent an amalgamation of two classes. FQM, floral quartet model; Se, sepals; Pt, petals; St, stamens; Ca, carpel; Ov, ovules. Figure adapted from Thomson and Wellmer (2019).

1.3. Floral Organ Specification and Development

How the activities of the floral homeotic factors lead to floral organ development has been a main focus area in the field of flower development over the last two decades. Genome-wide localisation studies and transcriptomics approaches have been used to elucidate the

target genes of the floral homeotic factors in Arabidopsis on a genome-wide scale (Wellmer *et al.*, 2004, 2006; Gómez-Mena *et al.*, 2005; Kaufmann *et al.*, 2010; Wuest *et al.*, 2012; O'Maoileidigh *et al.*, 2013; Pajoro, Madrigal, *et al.*, 2014; Chen *et al.*, 2018).These studies have shown that the floral homeotic proteins are bi-functional transcription factors and thus act as both repressors and activators of gene expression. From the genome-wide data, it appears as though these factors bind the binding sites of several thousand genes but only directly regulate a subset of them. This might be because the floral organ identify factors may require the presence of additional transcriptional regulators for their activity. In fact, proteomics approaches have led to the identification of additional transcription factors and epigenetic regulators that are associated with the MADS-domain protein complexes. Of the genes regulated by the floral organ identity factors, many encode transcriptional regulators that are involved in processes such as the control of the cell cycle and hormone response pathways as well as microRNAs and chromatin remodellers (Pajoro, Biewers, *et al.*, 2014; Chen *et al.*, 2018). The floral homeotic factors regulate hundreds of genes in order to bring about floral organ development. The transcriptomic studies and genome-wide binding analyses have shown that their target genes change throughout flower development as the floral organs develop (Ryan *et al.*, 2015). Furthermore, it has been demonstrated that the floral homeotic factors have two distinct function: the first is to activate genes with flower specific expression for floral organ development, while the second is to modify or suppress other genetic pathways in the plant (summarized in: Thomson and Wellmer, 2019). This will be discussed further in the next section.

1.4. Leaf to Flower Conversion

The flower is believed to be the defining feature for the evolutionary success of angiosperms. One aspect of angiosperm evolution that has been strongly supported by molecular evidence is that flowers are composed of highly derived leaves (Honma and Goto, 2001; Pelaz *et al.*, 2001; Theissen and Melzer, 2007). As described above, this concept was originally proposed by von Goethe in the late 18th century (von Goethe, 1790) and has garnered several lines of experimental evidence. The first line of evidence arises from mutants in which either A, B, and C class genes, or all E class genes are simultaneously inactivated. These mutant plants form structures in place of flowers that are entirely composed of leaf-like organs (Bowman,

Smyth and Meyerowitz, 1991; Ditta *et al*., 2004). Additionally, the ectopic expression of different combinations of floral organ identity genes (as predicted by the ABCE model) results in the transformation of rosette and/or cauline leaves into floral organs (Pelaz *et al.*, 2001; Honma and Goto, 2001). These veins of evidence provide solid support for the concept that flowers are composed of highly derived leaves. Although these results unequivocally showed that the floral homeotic genes are pivotal for the conversion of leaves into floral organs, how the corresponding transcription factors control this conversion is largely unknown.

Previous work by the Wellmer laboratory and by other groups aimed to understand how the floral homeotic transcription factora specify organ fate. To this end, a combination of gene perturbation assays, genome-wide localisation studies and computational analyses were used (Kaufmann *et al.*, 2010; Wuest *et al.*, 2012; O'Maoileidigh *et al.*, 2013; Pajoro, Madrigal, *et al.*, 2014). Results from these experiments showed that the floral organ identity factors indeed regulate genes with known flower-specific functions. For instance, AG controls the formation of the floral reproductive organs making it no surprise that it was shown to regulate *SUPERMAN* (*SUP*), *CRABS CLAW* (*CRC*) and *SPOROCYTELESS/NOZZLE* (*SPL/NZZ*) which are known regulators of carpel and stamen development (Ito *et al.*, 2004; Lee *et al.*, 2005, 2019; Liu *et al.*, 2009; O'Maoileidigh *et al.*, 2013). Furthermore, it was demonstrated that the floral homeotic factors regulate genes that have peak expression during leaf development (O'Maoileidigh *et al.*, 2013). Specifically, it was shown for AG that it suppresses the formation of trichomes, which is a hallmark of leaf development, on carpel valves (O'Maoileidigh *et al.*, 2013). O'Maoiléidigh *et al.* (2018) later demonstrated that this suppression depends on AG repressing activators of trichome initiation such as *GLABRA1* (*GL1*), and activating the expression of repressors of trichome development. It was also shown that AG controls responses to the phytohormone cytokinin, which is known to promote the formation of trichomes in leaves. Thus, the floral homeotic factors control floral organ formation not only by activating the expression of genes that are specifically required for floral organ formation but also by altering and in part suppressing the genetic programme for leaf development.

Among the regulators of leaf development targeted by the floral homeotic factors in Arabidopsis are genes that are involved in the control of organ polarity. Specifically, it was shown that *AG* genetically interacts with *KANADI1* (*KAN1*), the founding member of the

KANADI gene family (O'Maoileidigh *et al.*, 2013, Kerstetter *et al.*, 2001). *KAN1* specifies abaxial identity in both leaves and carpels, and encodes a GARP (for: Golden2, ARR-B and Psr1) transcription factor (Kerstetter *et al.*, 2001) . While it is already known that many of the known organ polarity genes, such as *KAN1*, are expressed in flowers and control aspects of floral organ formation, how they are regulated by the floral homeotic factors is largely unknown.

1.4.1 Control of Polarity in Leaves

While discussing the polarity genes and their relationship with flower development, it would be remiss not to discuss their fundamental and well-established roles in leaf development as well as briefly discussing how leaves themselves form.

Briefly, there are four stages that govern leaf development and morphogenesis. The first stage is characterised by the recruitment of cells from the peripheral zone of the SAM into incipient leaf primordia (Fig. 1.4A). The second stage involves the distal growth of the leaf primordia as well as abaxial-adaxial polarity establishment (Fig. 1.4B). During the third stage, the leaf blade is initiated and margin boundaries between the leaf blade and the petiole are established (Fig. 1.4C). Finally, in the fourth stage, the marginal meristem activity is terminated and this is followed by intercalary growth of the leaf in multiple directions (Fig. 1.4D) (Nakata and Okada, 2013; Du, Guan and Jiao, 2018).
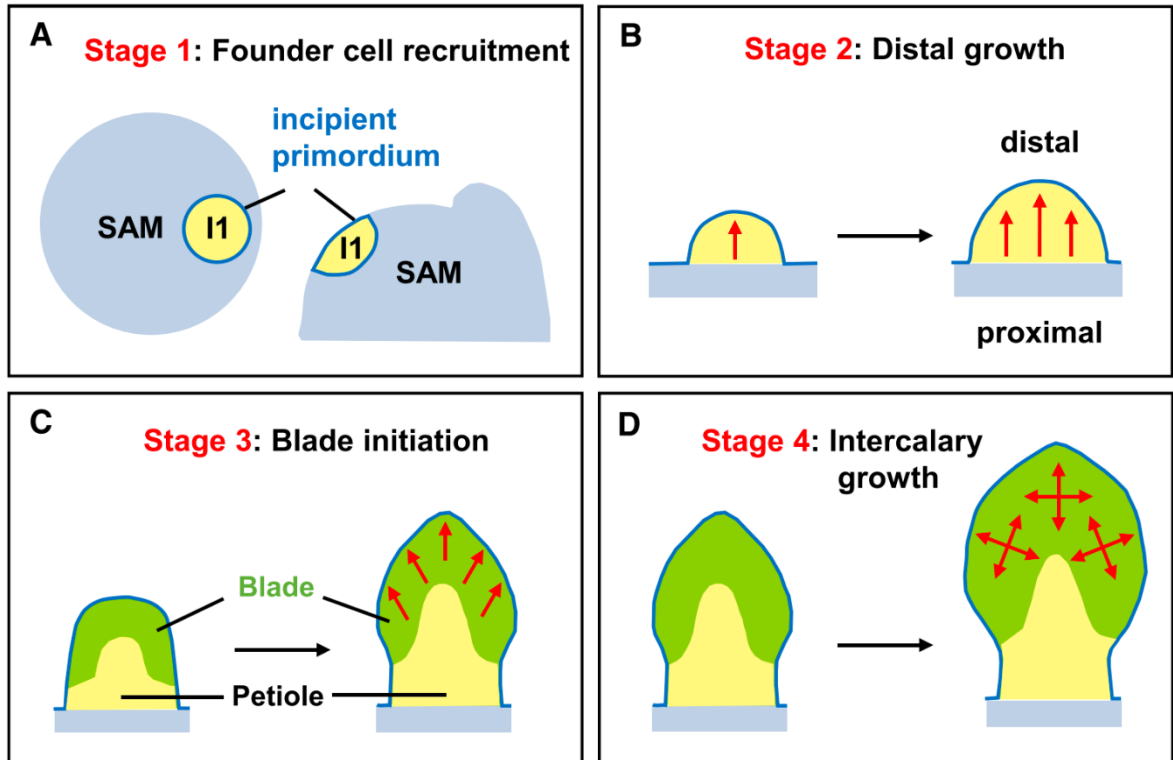
Figure 1.4: The four stages of leaf development.

(A) Founder cells are recruited from the SAM to the incipient primordium (I1**). (B)** This is followed by distal growth of the leaf (**C**). The blade and petiole regions are specified which is followed by leaf outgrowth. (**D**) The meristem activity is terminated and cell expansion occurs in the entire leaf blade. Figure taken from Du, Guan and Jiao (2018).

The stage of leaf development that is of particular importance for the research discussed in this thesis is that of abaxial and adaxial polarity specification. Most leaves are dorsiventrally flattened and develop clearly defined upper and lower surfaces (Kaplan, 2001). Light capturing is the specialisation of the adaxial or upper surface and the abaxial (lower surface) is specialised for gaseous exchange (Fig. 1.5A) (Kidner and Timmermans, 2010). The adaxial surface of true leaves form trichomes which in Arabidopsis are small, single-celled hair-like outgrowths. These trichomes are not present on the abaxial surface of leaves until the plant is in its adult stage (Uhrig and Hülskamp, 2010; Liu *et al.*, 2012; Pattanaik *et al.*, 2014).

The abaxial-adaxial polarity of leaves begins early on during founder cell recruitment. The portion of the leaf primordia that is closest to the SAM forms the adaxial domain, whereas the portion furthest from the SAM becomes the abaxial domain (Yamaguchi *et al.*, 2012) . The stem cells that form the developing leaf primordium are thought to carry a positional signal from the meristem to the patterning leaf. The concept of this positional signal originated due to classical microsurgical experiments by Sussex (1951). In these experiments, the emerging leaf was separated from the SAM resulting in an abaxialised radially symmetric leaf. This experiment lead Sussex to hypothesise that there was a signal from the SAM that promotes adaxial cell fate (Sussex, 1951). The true nature of this so-called 'Sussex signal' still remains unknown to scientists. However recent time lapse imaging experiments indicate that REVOLUTA (REV), a HD-ZIPIII transcription factor defining adaxial cell fate, is expressed in the oldest incipient primordium and that REV-expressing cells form the adaxial domain (Emery *et al.*, 2003; Caggiano *et al.*, 2017).

The adaxial polarity of the leaf has been shown to be established and maintained by a group of plant-specific homeodomain/leucine zipper (*HD-ZIP*) transcription factors (Mcconnell *et al.*, 2001). Whereas, the abaxial domain is established and maintained by *KAN* and *YABBY* family of transcription factors (Kerstetter *et al.*, 2001; Siegfried *et al.*, 1999). Once the adaxial-abaxial polarity of the leaf is established, it is maintained and strengthen by domain specific expression and mutual repression of numerous transcription factors and microRNAs (reviewed by Manuela and Xu, 2020).

Adaxial polarity is established and controlled by *REV* and related HD-ZIPIII transcription factors *PHAVOLUTA (PHV)* and *PHABULOSA (PHB)* which are all expressed on the adaxial side of the leaf (Fig. 1.5B) (Mcconnell *et al.*, 2001; Emery *et al.*, 2003). The expression domains of these genes are restricted by microRNA165 (miR165) and microRNA166 (miR166) which mediate the degradation of the HD-ZIPIII mRNAs. These microRNAs accumulate in a gradient with highest expression in the abaxial side of the leaf primordia (Fig. 1.5B) (Juarez *et al.*, 2004; Nakata and Okada, 2013). This results in a sharp HD-ZIPIII expression boundary observed in the adaxial domain (Skopelitis *et al.*, 2017). Additionally, *REV, PHV* and *PHB* physically interact with *HOMEOBOX-LEUCINE ZIPPER 3 (HAT3)* and *ARABIDOPSIS HOMEOBOX-LEUCINE ZIPPER PROTEIN 4 (ATHB4)* (Merelo *et al.*, 2016).

Expression of the HD-ZIPIII genes has been shown to be sufficient to define adaxial cell fate.

In gain of function HD-ZIPIII mutants, it was found that the HD-ZIPIII genes can escape inhibition by miR165/166 through mutations in their miRNA binding sites, resulting in adaxialized leaves. Whereas, loss of function *phb phv rev* triple-mutant plants form abaxialized leaves and exhibit loss-of-SAM phenotypes (Mcconnell *et al.*, 2001; Emery *et al.*, 2003). Adaxial cell fate also is refined by an additional transcription factor, ASYMMETRIC LEAVES2 (AS2) (Iwakawa *et al.*, 2007).

In a manner similar to adaxial cell fate specification, abaxial cell fate is controlled by antagonistic transcription factors and small RNAs. Abaxial identity is established by members of two gene families, termed *KANADI* and the *YABBY* (Emery *et al.*, 2003; Manuela and Xu, 2020). As mentioned above, the *KAN* genes encode members of the GARP family of transcription factors. Each of these genes is expressed in the abaxial side of the developing leaf (Kerstetter et al., 2001). *KAN* was originally identified in a screen looking for enhancers of the *crabs claw* mutation (Kerstetter *et al.,* 2001). Loss of function and gain of function *kan* mutations show that *KAN1* and other members of the *KAN* family cause abaxialisation and SAM termination (Kerstetter *et al.,* 2001).

The YABBY (YAB) family of transcription factors also contributes to abaxial polarity of the leaf. Initially, members of this gene family are expressed in the whole leaf primordium and are later restricted to the abaxial domain. Single mutants of *YAB* family members do not have leaf polarity defects, however, quadruple *yab1/2/3/5* mutants have radialized leaves indicating a high degree of functional redundancy with the gene family (Siegfried *et al.*, 1999).

Additionally, abaxial cell fate is also promoted by three redundant repressive AUXIN RESPONSE FACTORs (ARFs): ETTIN, ARF4, and ARF2 (Fig. 1.5B) (Pekker, Alvarez and Eshed, 2005). Furthermore, transacting short interfering RNAs (ta-siRNAs) perform a similar role to microRNAs in order to restrict abaxial determinants. The ta-siRNAs, generated via miR390 mediated cleavage, target *ETT*, *ARF2*, and *ARF4* expression. These ta-siRNAs are generated in the adaxial domain which causes the expression of the ARF genes to be restricted to the abaxial domain (Allen *et al.*, 2005).
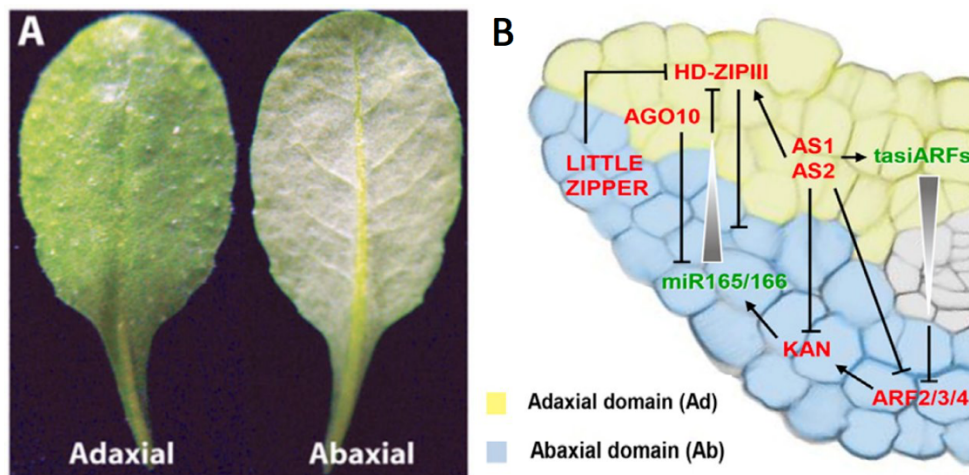
Figure 1.5: Adaxial-abaxial polarity specification in leaves.

(A) The adaxial side of an Arabidopsis leaf exhibits a dark green colour and carries numerous trichomes, whereas the abaxial side is a lighter green and has less trichomes. **(B)** Specification of abaxial-adaxial polarity in leaves is regulated by diverse transcription factors and small RNA gradients. Figure adapted from Chitwood *et al.* (2007) and Bar and Ori (2014).

1.5. MicroRNAs and their functions in flower development

MicroRNAs (miRNAs) are a class of small non-coding RNAs (approximately 17-24 nt in length) that post-transcriptionally regulate gene expression (Liu *et al.*, 2018). There are two mechanisms through which miRNAs can regulate gene expression: the first involves the binding of miRNAs to specific target RNAs, which marks them for degradation. The second mechanism for miRNA activity relies on decreasing the level of translation of the target mRNAs by interfering with the translation machinery (Borges and Martienssen, 2015).

MiRNA biogenesis in plants starts with the miRNA genes being transcribed by RNA polymerase II. This results in a long RNA that is called the primary-miRNA (pri-mRNAs) (Xie *et al.*, 2005). Pri-miRNAs are processed in the nuclease by DICER-LIKE1 (DCL1) which results in an imperfect stem-loop structure. This structure results in a miRNA/miRNA* duplex which is exported by HASTY from the nucleus to the cytoplasm (Dong, Han and Fedoroff, 2008). The mature miRNA then interacts with the ARGONAUTE

(AGO) proteins to form the RNA induced silencing complex (RISC). The miRNA* strand is often degraded in this process. The RISC complex then directs miRNA to its target mRNA. The target mRNA is then repressed by mRNA cleavage, translational inhibition or chromatin modifications (Borges and Martienssen, 2015).

1.5.1. The importance of miRNAs in plant development

MiRNAs have been recognised as key regulators of plant developmental processes. Many of the genes targeted by miRNAs are transcription factors which makes them key players in the gene regulatory networks controlling developmental events (Liu *et al.*, 2018). Some of the developmental processes that are regulated by miRNAs in Arabidopsis are outlined in Table 1.1.

For example, MIR156 plays a vital role in the transition from vegetative to reproductive growth. The levels of MIR156 gradually decrease with the age of the plant. This results in the upregulated expression of the SQUAMOSA PROMOTER BINDING-LIKE (SPL) transcription factors (Huijser and Schmid, 2011) (Xu *et al.*, 2016). These transcription factors are activators of *LFY* and *AP1* as well as MIR172. MIR172 targets *AP2* which results in the floral transition and activation of the floral homeotic genes (Aukerman and Sakai, 2004). Additionally, as mentioned in Section 1.41, miR165/166 are required forp restricting the expression of the HD-ZIPIII genes to the adaxial side during leaf development (Juarez *et al.*, 2004).

Chen *et al.* (2018) used genome-wide transcription factor binding data, as well as mRNA and miRNA expression data to understand the dynamic gene regulatory network that controls floral meristem development and organ differentiation. This research found that half of all annotated miRNA genes (167 out of 325) were regulated by at least one floral regulator. Of particular interest to this research is AG, which was shown to bind to the presumptive regulatory regions of 32 miRNA target genes. The work also identified novel feed-forward loops between the floral homeotic factors and other factors responsible for organ size and morphology. Future research will be required to experimentally prove these feedback loops which is why an accessible method of detecting individual miRNA is so important (Chen *et al.*, 2018).

Table 1.1: The target genes of conserved miRNAs in Arabidopsis and their functions.
Table adapted from Liu *et al.* (2018).

MiRNA	Target genes	Function
miR156/157	*SPL2/3/4/5/6/9/10/11/13/15*	Vegetive to reproductive transitions
miR159	*MYB33/65/101*	Leaf shape, flowering time and floral patterning
miR164	*CUC1/2, NAC1, ORE1*	Boundary formation during leaf and floral development
miR165/166	*PHV, PHB, REV, HB8, HB15*	Shoot meristem development, abaxial and adaxial polarity
miR172	*AP2, TOE1/2/3, SNZ, SMZ*	Flowering time and floral development
miR319	*TCP2/3/4/10/24*	Leaf morphogenesis and floral development

1.6. Experimental Aims

The work described in this thesis had two broad aims. The first aim was to address the existing knowledge gap on how leaves are converted into floral organs. To this end, I sought to study the function of genes that are known to control the shape and the polarity of leaves but are also known to be active during floral organ development. The genetic and molecular evidence outlined above suggests that an interplay of the organ polarity regulators and the floral homeotic transcription factors is important for shaping floral organs. Furthermore, these regulatory genes may be highly relevant in the context of floral evolution in that differences in their interactions may explain the astounding variations in floral morphologies found among different angiosperms. To better understand this interplay, I sought to employ gene perturbation assays to identify genes and pathways controlled by these regulators during floral organ development.

As the floral homeotic factors work in a combinatorial manner with other transcription factors and miRNAs to specify organ identities in flowers, the second aim of this Master's thesis was to establish a reliable and effective miRNA detection protocol. This detection protocol would then allow to investigate the interplay between the floral homeotic factors and selected miRNAs.

Chapter 2. Materials and Methods

2.1. Strains and Growth Conditions

2.1.1. Plant lines

Wild-type plants of accession Columbia (Col-0).

Wild-type plants of accession Landsberg *erecta* (L-*er*).

Transgenic plants of the following genotype: pAP1::AP1-AR p35S::GR-LhG4 6xpOp::AG-amiRNA *ap1-1 cal-1* (Thompson, 2017).

2.1.2. Plant Growth Media

Plants were grown in autoclaved soil composed of compost, perlite and vermiculite in a 3:1:1 ratio. Plants were treated at 4°C for 3 days to synchronise germination before being placed in a plant room. The plants were grown under a constant white fluorescent light (6,000 K) at 20°C.

2.1.3. Bacterial Strains

- *E. coli* Stb12 competent cells
- *Agrobacterium tumefaciens (Agrobacterium)* GV2260 cells

2.2. Cloning and Genotyping

2.2.1 Plasmid Miniprep extraction

Cultures of transformed *E. coli* colonies were grown in 5 ml of LB at 37°C overnight in an orbital shaker with the appropriate selective antibiotic before being centrifuged at 4,500 r.p.m. for 10 min. The plasmids were miniprepped using the OMEGA E.N.Z.A Miniprep Kit following the manufacturer's instructions.

2.2.2. PCR product purification

PCR products were purified using the EZNA Cycle Pure kit (Omega BioTek) according to the manufacturer's instructions.

2.2.3. Gel Electrophoresis

PCR products were run out on 1% (w/v) agarose gels. The gels were made from 60 ml TAE buffer, 0.6 g agarose and 7 µl ethidium bromide. The gels were visualized and photographed using a UV transilluminator.

2.2.4. Quantification of nucleic acid concentrations

The concentration and quality of DNA and RNA were determined using a Nanodrop 1000 spectrophotometer. The Nanodrop spectrophotometer was 'blanked' with the solution used to dissolve the nucleic acid.

2.2.5. Plant genomic DNA extraction

Edwards DNA preparation was used for crude extraction of genomic DNA for genotyping purposes. The protocol is based on the method described by Edwards *et al.* (1991) with minor changes. Specifically, to ensure a consistent amount a plant tissue, a small piece of tissue was collected using a hole punch.

2.2.6. Preparation of chemically competent E. coli cells

Competent cells were prepared according to the protocol established by Inoue *et al.* (1990).

2.2.7. Transformation of E. coli

E. coli transformations were carried out using the heat shock protocol. Competent cells were thawed on ice and mixed with 5 µl of the ligation product. The cells were chilled for 10 minutes before being heat shocked for 45 seconds at 42°C. The cells were then incubated in the orbital shaker at 37°C for 1 hour in 1 ml of LB medium. They were then centrifuged at 5,000 rpm for 2 minutes. 500 µl of LB medium was discarded before the pellet was resuspended. 100 µl of solution was spread on a LB agar plate with the required antibiotic.

2.2.9. Colony PCR of E.coli

To ensure the presence of the required inserts in heat shock transformed *E. coli* colonies, single colonies were picked and suspended in 20 µl LB. 1.5 µl of this suspension was then used in genotyping PCRs.

2.2.10. Oligonucleotide design

Oligonucleotides were designed using the OligoAnalyzer tool designed by Integrated DNA technologies. All oligonucleotides were designed to ensure a minimum amount of hairpin structures and dimerization, to have a GC content between 40-60% as well as possessing melting temperature between 50-60°C.

Oligonucleotides for quantitative PCR were designed using NCBI Primer-Blast with the following specifications. The primers were designed to be between 70 bp and 200 bp long as well as having a melting temperature between 60-63°C. They were also designed to span an exon-exon boundary.

The quantitative PCR oligonucleotides were then subjected to a standard curve test to ensure they were efficient. Oligonucleotides were only used if they had a range of 90-110% with less than 0.99 for the R^2 of the curve.

Oligonucleotides used for microRNA detection were designed using the protocol described in Chen *et al.* (2005).

2.2.11. Sanger Sequencing of DNA

The inserts were sequenced by GATC Biotech to ensure no mismatches occurred during the PCR amplification. The sequences were compared to the expected sequences using the ApE plasmid editor software.

2.2.12. RNA extraction

2.2.12.1 Total RNA extraction

Total RNA was isolated from plant material using the Spectrum Total Plant RNA Kit (Sigma Aldrich) according to the manufacturer's instructions. On-column DNaseI digestion was performed on samples to remove as much residual genomic DNA as possible. RNA quality was measured using a Nanodrop 1000 spectrophotometer to check OD260/230 and OD260/280 ratios. Purified RNA was stored at -80°C.

2.2.12.2 RNA extractions using Trizol

Total RNA was isolated from frozen plant material using Trizol based on the method described by Toni *et al.* (2018). This method utilises a second chloroform extraction step as

well as additional ethanol washes to enhance RNA purity. Briefly, the plant tissue was homogenised in 500 µl Trizol and let sit at RT for 3 minutes. 100 µl chloroform was added and shaken rigorously by hand for 15 s and allowed sit for 3 minutes. The reaction tube was then centrifuged at 4°C at 12,000 x *g* for 15 minutes. The upper aqueous layer was then transferred into new reaction tube with 100 µl chloroform for a second chloroform extraction. The RNA was precipitated using 250 µl isopropanol. This was centrifuged at 4°C 12,000 x *g* after sitting at room temperature for 10 minutes. The supernatant was removed, and the pellet was washed three times using 1 ml 75% ethanol. The tubes were heated at 65°C for 2 minutes to evaporate the remaining ethanol. 40 µl nuclease free water was used to resuspend the pellet. The tubes were then heated at 65°C for 2 minutes to stabilise the RNA. The RNA quality and storage was the same as described in Section 2.2.12.1.

2.2.13. cDNA synthesis

cDNA was generated from total RNA using the Thermo Scientific RevertAid First Strand cDNA Synthesis Kit following the manufacturer's instructions. RNA extraction from the method described in Section 2.2.12.2 was treated with DNase I prior to cDNA extraction. Unless otherwise stated, Oligo(dT) 18 (Thermo Scientific) was used as was 500 ng of total DNA and 0.5 µl Reverse transcriptase for each 20 µl reaction. The cDNA was diluted and 2 µl was used for the quantitative PCR reaction.

2.3. Quantitative PCR

Quantitative PCR was performed with a Light Cycler 480 (Roche) and the SYBR Green Master I reagent (Roche). Each reaction contained 2 µl of a 1:5 dilution of cDNA, 1 µl of 5 µM primer mix, and 5 µl of SYBR Green Master I, and 2 µl ultra-pure H_2O. Plates were centrifuged prior to insertion into the Light Cycler 480. An annealing temperatures of 60°C was used and an equivalent time of 60 s per 1 kb of template length was given to generate the amplicons.

The enrichment was calculated relative to a reference gene using the double delta Cp analysis. For each locus analysed, the enrichment was calculated as follows: $2^{Cp(REF)-Cp(GENE)}$, where Cp is the crossing point calculated by the LightCycler 480, Cp(REF) is the Cp value for the chosen reference gene and Cp(GENE) is the Cp value for the chosen target gene. The

reference gene used for RT-qPCR was DM-242/DM-243 (AT1G13320), which was chosen from Czechowski *et al.* (2005).

2.4 MicroRNA detection

2.4.1 MicroRNA detection using stem-loop RT-qPCR

Each reaction contained 0.5 μM of each forward and reverse primer, 0.1 μM Universal ProbeLibrary Probe #21, 1x LightCycler® TaqMan® Master, and 2 μl of cDNA totalling 20 μl. Amplification curves were generated with an initial denaturing step at 95°C for 10 minutes, followed by 45 cycles of 95°C for 5 seconds, 60°C for 15 seconds, and 72°C for 1 second. Results were analysed using the double delta Cp analysis as described in Section 2.3.

2.4.2 MicroRNA detection using the Mir-X miRNA First-Strand Synthesis and Mir-X miRNA qRT-PCR TB Green Kit

MicroRNAs were also detected using the Mir-X miRNA First-Strand Synthesis and Mir-X miRNA qRT-PCR TB Green Kit following the manufacturer's instructions (Takara Bio, Japan).

2.6 Treatment of the floral induction system

2.6.1. Dexamethasone treatments

Inflorescenes of approximately 4-week old pAP1::AP1-AR p35S::GR-LhG4 6xpOp::AG-amiRNA *ap1-1 cal-1* plants were treated with an aqueous solution containing 10 μM dexamethasone, 0.1% (v/v) ethanol, and 0.015% (v/v) Silwet L-77. For mock-treated samples, the dexamethasone was omitted from the treatment solution.

2.6.2 Dihydrotestosterone treatments

Inflorescenes of approximately 4-week old pAP1::AP1-AR p35S::GR-LhG4 6xpOp::AG-amiRNA *ap1-1 cal-1* plants were treated with aqueous solutions containing 100 μM dihydrotestosterone (DHT), 0.1% (v/v) ethanol, 2.5 mg/ml (2-Hydroxypropyl)-β-cyclodextrin, and 0.015% (v/v) Silwet L-77 by dropping the solution onto the inflorescences

with a plastic pipette. For mock-treated samples, the dihydrotestosterone was omitted from the treatment solution.

2.6.3 Floral Induction System Tissue Collection

Inflorescence tissues from plants of the floral induction system were collected using sterile 22 surgical blades under a stereo microscope. To this end, only the upper sections of the 'curds' were harvested as they contain the meristematic tissue. The tissue was then immediately placed in 1.5 ml reaction tubes and submerged in liquid nitrogen. Samples were stored at -80ºC until further use.

Chapter 3. Results

As mentioned in Section 1.4, recent work in the Wellmer laboratory has started to uncover the developmental processes that are directly regulated by the floral homeotic factors AP1, AP3, PI, and AG. This previously published work (Wuest *et al*., 2012; O'Maoileidigh *et al*., 2013) showed that these genes play a vital role in flower developmental pathways as expected. However, they were also shown to regulate organ patterning and leaf developmental programmes. This previous work lays the foundations for the research described in this chapter in which AG was used a proxy to examine the interplay between the floral homeotic factors and the genes governing organ polarity.

3.1.1 Identification of AG *regulated leaf polarity genes*

Table 3.1 summarises this work in relation to AG's interactions with the leaf-specific organ polarity genes. The primary function for the genes listed in the table is to specify abaxial/adaxial polarity in leaves. This table summarises previous work, namely ChIP-seq analysis and microarray experiments for AG, carried out by Dr. Diarmuid O'Maoileidigh and colleagues. To this end, synchronised floral buds at stage 5 (stages according to Smyth *et al.,* 1990) were collected from the pAP1::API-GR pAG::AG-GFP *ap1-1 cal-1 ag-1* line from four biologically independent samples. ChIP-seq was then performed which identified 1,487 high confidence binding sites for AG-GFP. This binding data was also compared to genome wide binding data for KAN1 in leaves (see Tab. 3.1).

In order to identify genes regulated by AG, the null mutant allele *ag-1* was introduced into the floral induction system (FIS). For context, the FIS was developed to allow for the collection of sufficient amounts of plant tissue to study specific developmental stages. This system is based on the *ap1 cal* double mutant plant. In an *ap1 cal* double mutant, there is a massive over-proliferation of inflorescence-like tissue which results in a cauliflower-like appearance (Ferrandiz et al., 2000). Flower development can be synchronised in this background by expressing a translational fusion between *AP1* and the rat glucocorticoid receptor (GR) ligand binding domain (denoted: AP1-GR). Treatment of pAP1::AP1-GR inflorescences with the glucocorticoid dexamethasone leads to the transformation of the inflorescence-like meristems into floral meristems, therefore resulting in synchronised flower development (Wellmer *et al.*, 2006).

Inflorescence tissue from individual plants was collected into separate tubes immediately before the induction of flower formation as well as 2.5 and 5 days after dexamethasone treatment. Subsequently, these plants were grown, and the resulting flowers were examined to identify plants that exhibited a loss of reproductive floral organs and thus were in all probability homozygous for the *ag-1* allele. Four biologically independent samples for each time-point were then used to compare the gene expression profiles of *ag* mutant flowers to those of wild-type flowers at different developmental stages. This led to the identification of 1,047 genes, several of which are genes involved in the leaf developmental process.

This work by O'Maoileidigh *et al.* (2013) was compared with data from RNA-seq experiments performed by Dr. Bennett Thomson (Thomson, 2017). The latter work used a pAP1::AP1-AR *ap1-1 cal-1* flower induction system. This systems functions in a similar manner to the pAP1::AP1-GR system (described above), however, the GR portion of the fusion has been replaced with the human androgen receptor (AR). The resulting AP1-AR fusion protein is activated when plants are exposed to dihydrotestosterone (DHT) resulting in the synchronised-induction of flowering. This line was combined with a p35S::GR-LhG4 6xpOp::AG-amiRNA construct, which allows for the stage specific down-regulation of *AG* activity. This system works as follows: the chimeric GR-LhG4 transcription factor is located in the cytoplasm until a DEX solution is applied to the inflorescences of the plants, at which point it translocates to the nucleus and binds the 6xpOp promoter, activating the transcription of the amiRNA precursor, which is then processed into the functional amiRNA and participates in the degradation of its target endogenous *AG* mRNA. The amiRNAs used in this study were previously developed and validated by Dr. Diarmuid O'Maoileidigh and Dr. Samuel Wuest in the Wellmer laboratory (Wuest *et al.*, 2012; O'Maoileidigh *et al.*, 2013).

Analysis of the data shown in Table 3.1 indicates that the majority of leaf organ polarity genes listed have binding evidence with *AG*. The differential expression data correlates with the binding data for a few genes such as *CUC1* and *PHB* (see Tab. 3.1). This could indicate that *AG* is regulating these genes during flower development. The RNA-seq data performed by Dr. Bennett Thomson (Thomson, 2017) examined the stage-specific downregulation of *AG* on the Arabidopsis genome at stage 3, stage 5 and stage 8 of flower development. Figure 3.1 highlights the effect of *AG* downregulation on the leaf genes from Table. 3.1. The differential gene expression is minor for the majority of genes examined. However, there are larger gene expression changes for *AF4*, *AS2* and *CUC1*. An important caveat of this RNA-

seq data is that it was only performed with two biological replicates. Therefore, a third biological replicate would be needed to draw any conclusive results.

Table 3.1. Summary of evidence for AG regulation of organ polarity genes in this study.

Cells are colour-coded to aid visualisation. Yellow cells represent positive results.

Alias	AGI	Differentially expressed? (microarray) O'Maoileidigh et al. (2013)	Differentially expressed? (RNA-seq) Thomson (2017)	Binding evidence? (ChIP-seq) AG O'Maoileidigh et al. (2013)	KAN Merelo et al. (2013)
KAN	AT5G16560	No	Yes	No	yes
KAN2	AT1G32240	Yes	No	Yes	yes
KAN4	AT5G42630	Yes	No	Yes	No
DRN	AT1G12980	No	No	No	No
DRNL	AT1G24590	No	No	Yes	No
AS1	AT2G37630	No	No	Yes	No
AS2	AT1G65620	No	Yes	No	Yes
CUC1	AT3G15170	Yes	Yes	Yes	No
LOB	AT5G63090	No	No	Yes	No
REV	AT5G60690	Yes	No	Yes	No
PHV	AT1G30490	No	No	Yes	No
PHB	AT2G34710	No	Yes	Yes	Yes
miR165	ATIG01183	No	No	Yes	No
miR166	AT2G46685	No	No	No	Yes
ETT	AT2G33860	No	No	Yes	Yes
ARF4	AT5G60450	No	No	No	Yes
ARF2	AT5G62000	No	No	No	Yes
ATHB-4	AT2G44910	No	No	Yes	No
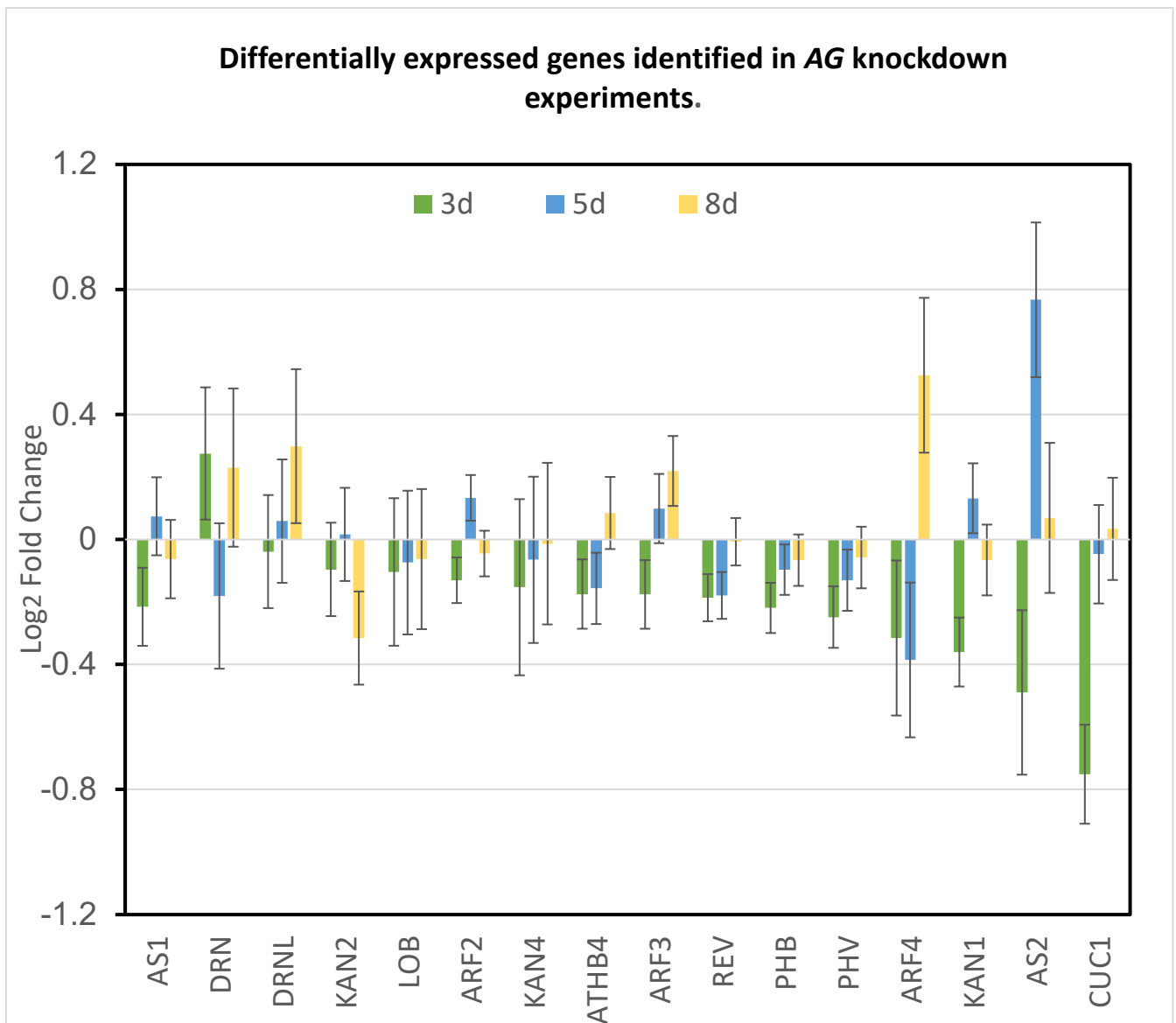
Figure 3.1: Differentially expressed leaf polarity genes identified in AG knockdown experiments. Log_{10} box plots of normalised transcript abundances, from flowers collected 24 hours after AGamiR$^{\text{DEX}}$ induction, at 3 (**A**), 5 (**B**), and 8 (**C**) days. Error bars represent standard deviations across two biological replicates. RNA-seq data provided by Dr. Bennett Thomson.

3.1.2 Genetic interaction between AG and the KANADI family

Table. 3.1 highlights that the majority of leaf genes are bound by *AG* or differentially expressed with *AG* perturbation. One family of particular interest is the *KAN* family of transcription factors which are required for abaxial identity in leaves and carpels. Previous research has shown the importance of the *KAN* family in specifying abaxial/adaxial polarity in carpel development. For example, double mutants of *kan1 kan2* plants result in gynoecia with adaxial cell types on their abaxial axes (Eshed et al., 2001), Additionally, *kan4* mutants result in ovule polarity defects (Kelley et al., 2009). Given this information, *AG* appears to promote the specification of the adaxial/abaxial axes of carpels and ovules in flower development by directly activating the *KAN* family of transcription factors.

As *AG* appears to regulate the *KAN* family to specify aspects of gynoecium development, *AG* and *KAN1* were examined to see if they genetically interact. To investigate this, Dr. Diarmuid O'Maoileidigh and Dr. Darragh Stewart examined plants mutant for both *AG* and *KAN1*. A *kan1* mutant gynoecium results in some tissue outgrowths (Fig.3.2C). However, these outgrowths are accentuated when *AG* is perturbed in *kan1* mutants (Fig.3.2D). Additionally, numerous trichomes form on the carpel valves of a *kan1* mutant flower with *AG* downregulation (Fig. 3.2E). As the double mutant has a stronger phenotypic result, this indicates that *KAN1* and *AG* genetically interact. It was also shown that *PHV*, *KAN2* and *CRC* transcriptionally respond to the perturbation of *AG*. This was shown by examining $\log_2$-transformed expression ratios from microarray experiments following an amiRNA-dependent down-regulation of *AG* (Fig. 3.2B).

Because *AG* and *KAN1* were shown to interact genetically, it was hypothesized that these two transcription factors may act together in the control of specific target genes. To test this, data from genome-wide localization studies for AG (O'Maoileidigh *et al.*, 2013) and those conducted for KAN1 (Merelo *et al.*, 2013) were compared. This analysis revealed 472 genes whose promoter regions are bound by both AG and KAN1 (Fig. 3.2A). To investigate whether this overlap was statistically significant, the representation factor and the exact hypergeometric probability of this occurring was calculated. The representation factor is calculated by dividing the number of overlapping genes by the expected number of overlapping genes from two independent groups. The representation factor for the data in

Fig. 3.2A was calculated to be 3.5. A representation factor over 1 indicates more overlap than expected for two independent groups. Additionally, a hypergeometric probability test was also performed to calculate the probability of this overlap occurring by chance. The p-value calculated for this data was $p < 7.113e\text{-}129$. This indicates that the observed overlap between the datasets (i.e., 472 genes) is highly significant. This high enrichment in common targets is especially noteworthy given that the ChIP-seq experiments for AG and KAN1 were done using very different tissue samples, namely early-stage flowers in the case of AG and rossette leaves in the case of KAN1.
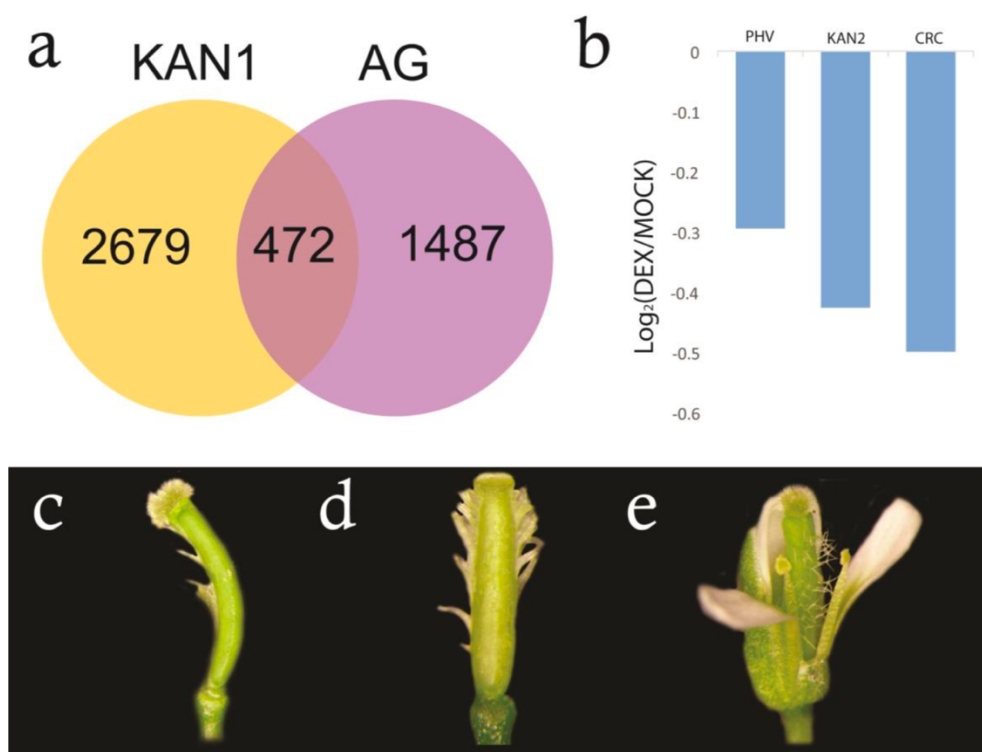
Figure 3.2: Interplay of floral homeotic factors and organ polarity regulators.

(A) Overlap of genes bound by the floral homeotic factor *AG* and the organ polarity regulator *KAN1*, as determined by ChIP-seq analysis. **(B)** Transcriptional response of organ polarity genes to *AG* perturbation. Log$_2$-transformed expression ratios from microarray experiments after an artificial microRNA-mediated knockdown of *AG* are shown. **(C)** A *kan1* mutant gynoecium with some tissue outgrowths on the sides. **(D)** A *kan1* mutant gynoecium after *AG* perturbation. Much stronger tissue outgrowths were observed when compared to the

gynoecium shown in panel c where *AG* functioned normally. **(E)** A *kan1* mutant flower after *AG* perturbation. Numerous trichomes form on carpel valves. In contrast, a perturbation of *AG* in a wild-type background leads to a much weaker phenotype (only few trichomes form; data not shown). Figure was provided by Prof. Frank Wellmer.

As the overlap of genes bound by AG and KAN1 was highly significant, the common target genes were analysed for enriched and under-represented Gene Ontology (GO) terms. To this end, GO terms in the category 'biological process' were investigated and their occurrence in the lists of common target genes was compared to their genome-wide distribution using a two-sided Fisher's exact test. GO terms that had an adjusted false discovery rate (FDR) of < 0.05 were judged as having a statistically significant distribution in the dataset. The three most highly enriched GO terms among the common AG/KAN1 target genes include among others '*Response to continuous far red light stimulus', 'Sucrose transport'*, and *'Radial pattern formation'* (see Tab. 3.2). In addition, GO terms relating to hormone responses (jasmonic acid and brassinosteroids, respectively) and the control of developmental processes are over-represented among the joint target genes (Tab. 3.2).

Table 3.2. Gene Ontology terms significantly enriched among the genes identified as targets of both AG and KAN1 from the ChIP-seq datasets. The fold enrichment values and false discovery rates (FDR) are listed for each GO term.

GO Term	Fold Enrichment	FDR
Response to continuous far red light stimulus by the high-irradiance response system	> 100	1.98E-02
Sucrose transport	28.81	2.43E-02
Radial pattern formation	26.19	2.82E-02
Regulation of cellular carbohydrate metabolic process	15.68	1.99E-02
Jasmonic acid mediated signalling pathway	13.52	4.78E-05
Brassinosteroid mediated signalling pathway	12.59	3.17E-02
Shoot system development	3.42	1.74E-02
Plant organ development	3.05	1.35E-02
Regulation of transcription, DNA templated	2.56	8.28E-04

3.1.3. Response of Leaf Polarity Genes to AG *Perturbation*

As outlined above, AG appears to function with KAN1 to specify organ polarity in the gynoecium. I, therefore, examined the regulation of *KAN* genes by AG by monitoring the transcriptional response of organ polarity genes to a specific down-regulation of *AG*.

To this end, an pAP1::AP1-AR p35S::GR-LhG4 6xpOp::AG-amiRNA line was used. This line will be referred to hereafter as FIS-AR AG-amiR$^{\text{DEX}}$. As described above, this line utilises the DHT responsive pAP1::AP1-AR *ap1-1 cal-1* (denoted as FIS-AR). This line was initially developed by Dr. Andrea Raganelli in the Wellmer laboratory. It was crossed with a DEX-inducible AG-amiRNA line developed and validated by Dr. Diarmuid O'Maoileidigh and Dr. Samuel Wuest in the Wellmer laboratory (Wuest *et al.*, 2012; O'Maoileidigh *et al.*, 2013). This allows for the synchronisation of flowering by the addition of DHT as well as stage-specific *AG* downregulation through DEX application.

The FIS-AR AG-amiR^{DEX} plants were grown at 16-18°C under constant illumination until they had bolted and the stem had extended more than 2 cm. The plants were transferred to a warmer temperature (20-22°C) and left for 24 hours before treatment. The DHT solution was used to saturate the inflorescence-like meristematic tissue characteristic of *ap1-1 cal-1* plants until they turned a darker green. After 2, 4 and 7 days, the floral buds were treated once with a 10 μM DEX solution, or a mock solution excluding DEX, and the top layer of tissue was collected 24 hours later. This results in collecting tissue at stages 3, 5 and 8 of flower development (Fig. 3.3) (stages according to Smyth *et al.*, 1990). These stages were chosen as they correlate with the stage-specific *AG* perturbation experiments performed by Dr. Bennett Thomson in Section 3.1.1. Additionally, these are landmark stages in flower development. Stage 3 corresponds to sepal primordia appearing on the flanks of the floral meristem, stage 5 is when petal and stamen primordia become visible and at stage 8, the gynoecium and stamens rapidly develop and elongate (Smyth, 1990).

Total RNA was extracted from these samples and converted into cDNA. RT-qPCR analysis of cDNA was performed and analysed using the double delta Cp analysis method (Fig. 3.3). The Cp values for the RT-qPCR were normalised to the reference gene (*At4g34270*) which was chosen from Czechowski *et al.* (2005). Furthermore, all the primer sets used for this study were subject to a standard curve test to check for efficiency.
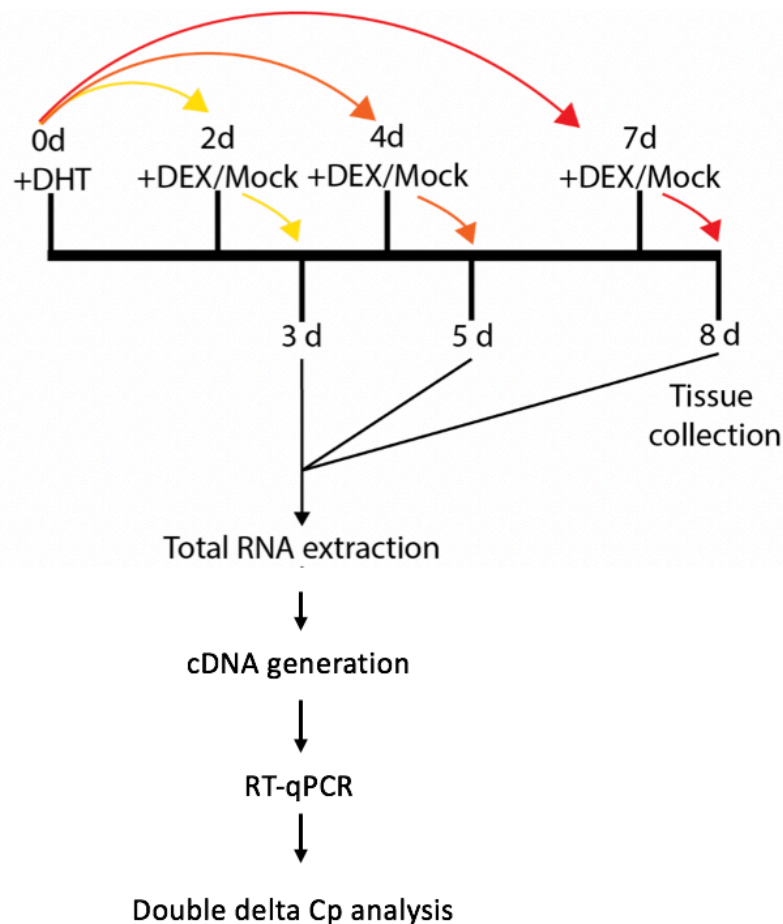
Figure 3.3: Experimental workflow for effect of AG perturbation on organ polarity genes. Inflorescences of FIS-AR AG-amiR$^{\text{DEX}}$ plants were treated with 500 μM DHT, and subsequently treated for 24 hours with a solution containing 10 μM DEX before tissue collection at the given time-points. After total RNA extraction and quality control, cDNA was generated and RT-qPCR was performed.

The results shown in Fig. 3.4 are the mean of three independent biological replicates, and two technical replicates for each stage being tested. The effect of *AG* down-regulation on organ polarity genes was examined in stage 3 flowers (Fig. 3.4A), stage 5 flowers (Fig. 3.4B) and stage 8 flowers **(**Fig. 3.4C**)**. The results show that *AG* transcript levels were shown to be reliably reduced to ~20% of those in mock-treated plants after 24 hours from DEX treatment. This indicates that the DEX-induced AG-amiRNA is working reliably in each experimental stage. While the expression of the differentially expressed genes (DEG) varies from each stage of flower development, *PHV* transcript levels are most striking in each developmental

stage. *PHV* transcript levels are continual down-regulated in each stage with the largest downregulation to ~65% in stage 8 floral tissue. This result is consistent with the transcriptional response of *PHV* to *AG* perturbation as determined through microarray analysis in Fig. 3.2B. However, the microarray analysis indicates a strong transcriptional response of *KAN2* to *AG* perturbation. This was relatively minor in stage 5 and stage 8 of flower development when examined in Fig. 3.4B and C. It is down-regulated to approximately 65% in stage 3 flowers with very small standard deviation evident by the error bars (Fig. 3.4A). Previous stage-specific *AG* perturbation experiments performed by Dr. Bennett Thomson (Thomson, 2017) (Fig. 3.1) did not report *KAN2* as a DEG at stage 3 of flower development.

There is a large transcriptional response of *PHB* to *AG* perturbation in stage 5 of flower development (~1.5 fold change). However it is evident by the error bars that there is a large standard deviation and that these results are not reliable.

One gene included in these RT-qPCR experiments was *KNUCKLES (KNU). KNU* is directly activated by AG at stage 6 of flower development. *KNU*, which encodes a C2H2-zinc finger transcription factor (Payne et al. 2004), then represses *WUSCHEL* (*WUS*), a gene that is required for stem cell maintenance (Sun *et al.*, 2009), This results in the termination of stem cell proliferation resulting in determinate structures (Sun et al., 2009). Therefore, *KNU* was included as a positive control in this experiment as it is directly target gene of AG. The expression of *KNU* is somewhat down-regulated (-90%) in stage 8 of flower development. The lack of a larger effect of *AG* perturbation on *KNU* expression could be due to the residual *AG* expression. It also could be due to the fact that, at stage 8 of flower development, KNU binds regulatory elements of *AG* and represses its activity (Shang, Ito and Sun, 2019).

A Effect of AG downregulation on organ polarity genes in stage 3 flowers

B Effect of AG downregulation on organ polarity genes in stage 5 flowers

C Effect of AG downregulation on organ polarity genes in stage 8 flowers
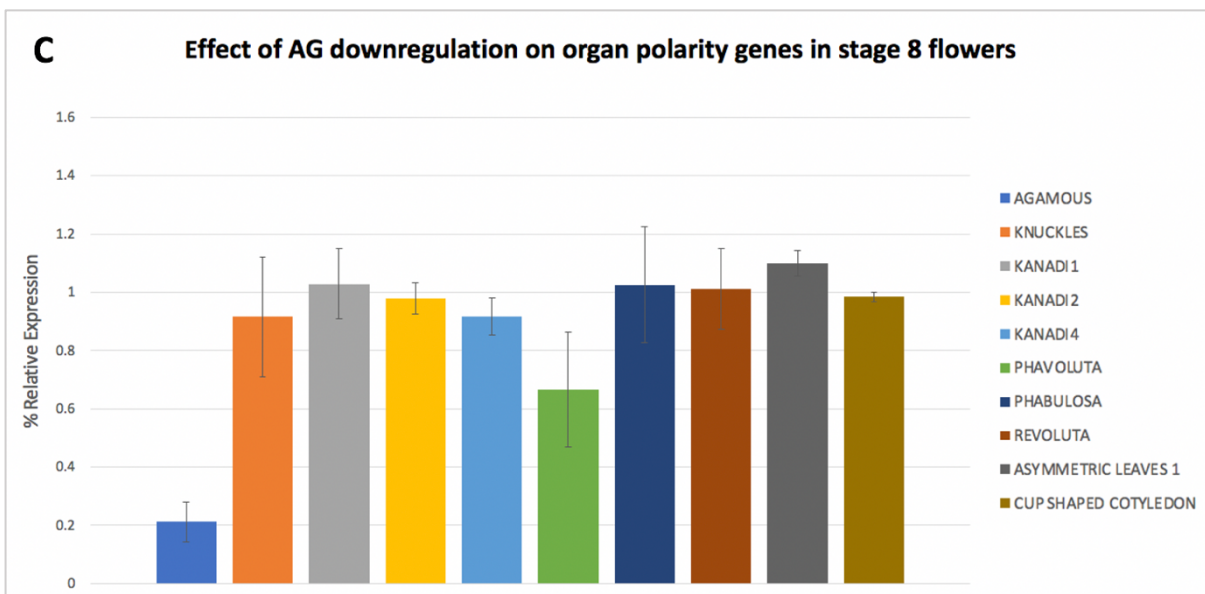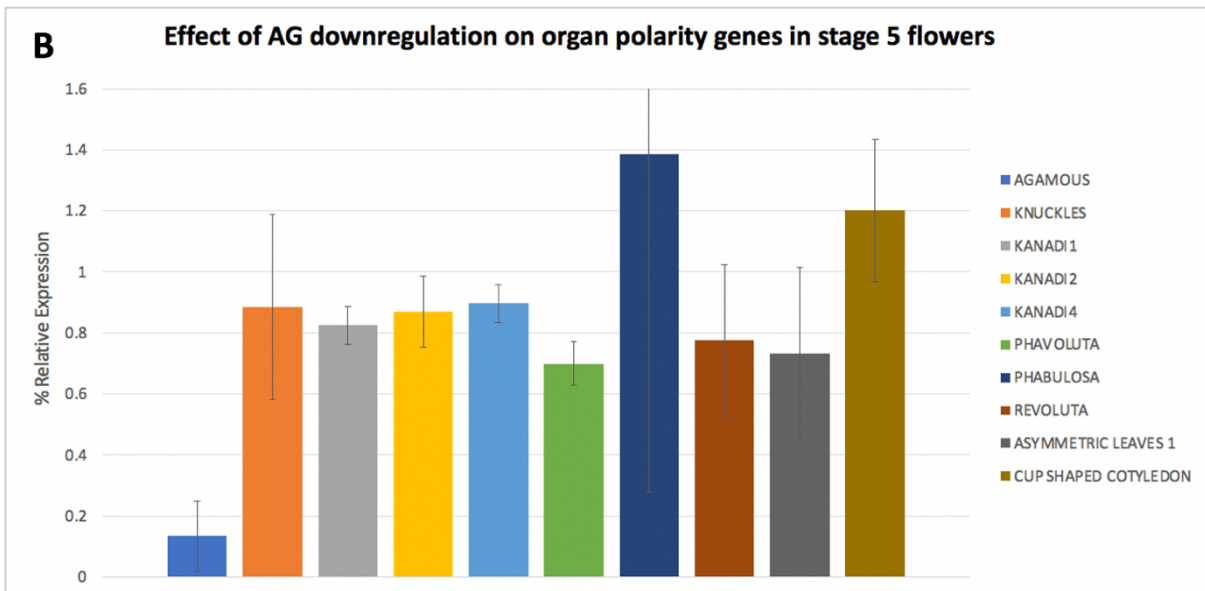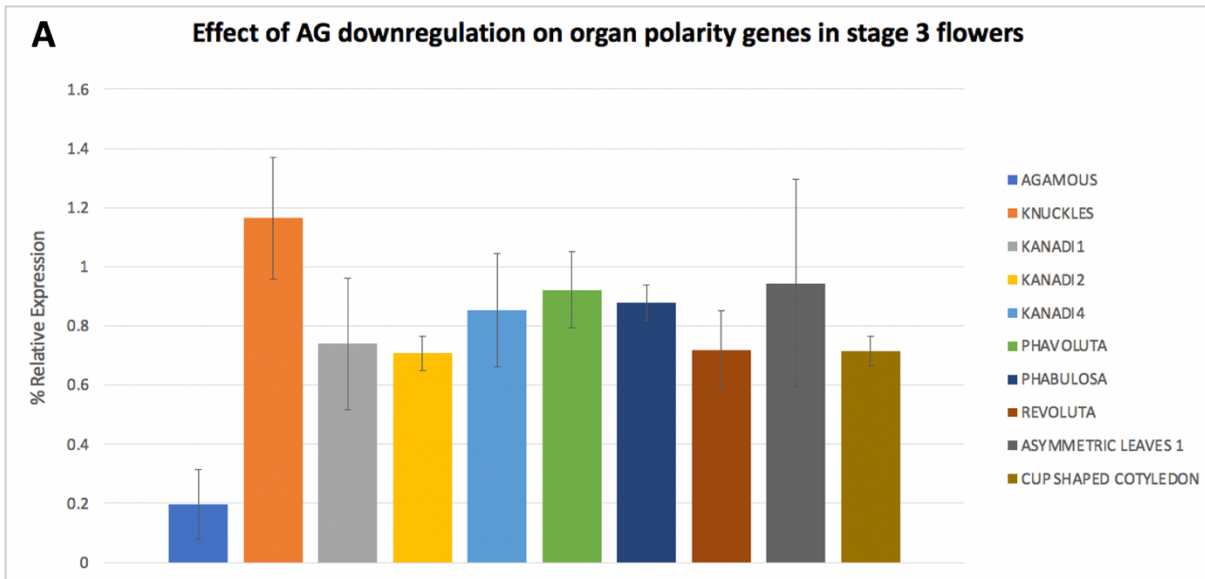
Figure 3.4: Effect of *AG* down-regulation on leaf polarity genes.

(**A-C**) Results of RT-qPCR experiments in which the effects of an *AG* down-regulation on the expression of leaf polarity genes was tested in (**A**) stage 3 flowers, (**B**) stage 5 flowers, and (**C**) stage 8 flowers. Relative expression values were calculated using the Double Delta Cp analysis method. Values represent the mean of three biological replicates. Two technical replicates were performed for each sample. Error bars represent standard deviations.

3.2. MicroRNA detection protocol

As discussed in Section 1.6, the second aim is to establish a reliable and effective protocol that enables the detection of endogenous microRNAs using RT-qPCR. Efficient and reliable detection of miRNAs is an essential step towards understanding their roles in specific tissues and cells. Less abundant miRNAs routinely escape detection with standard technologies, such as cloning, Northern hybridization, and microarray analysis (Chen *et al.*, 2005). These miRNAs can be detected by next generation sequencing however this tends to be time consuming, expensive and requires a high RNA input (Chugh and Dittmer, 2012).

Sensitive reverse-transcription quantitative PCR (RT-qPCR) methods combine high speed, throughput, sensitivity, specificity, affordability, and are often the method of choice for researchers (Chen *et al.*, 2005). Standard and quantitative PCR methods require a template that is at least twice the length of either the specific forward or reverse primers. These primers are typically ~20 nt in length. Therefore, this results in a minimum target length that is approximately 40 nt which makes miRNA too short for standard RT-qPCR method (Kramer, 2011).

In 2005, Chen *et al.* circumvented this problem through the development of a stem-loop qPCR method as a way to detect mature miRNAs. This is a two-step process that utilises a stem loop primer that binds to the 3' end of the mature miRNA. This is then reverse in a pulsed RT reaction. The resulting cDNA is then amplified with a miRNA specific forward primer and a universal reverse primer. A miRNA-specific TaqMan® probe is used and the

fluorescence is measured to quantify mature miRNA level. However, TaqMan® probes have been optimised for mammalian miRNA and each probe is specific to an individual miRNA (Fig. 3.5A). This makes it very costly for laboratories and not amenable for high-throughput analysis of a large number of miRNAs. This led to a more economical miRNA quantification method that uses the stem-loop RT-qPCR method combined with Universal ProbeLibrary (UPL) technology (Wu *et al.*, 2007). This method uses stem loop primers designed according to Chen et al., however they are modified to include the universal ProbeLibrary Probe #21 sequence binding site (Fig. 3.5B). The cDNA is subsequently amplified using a miRNA specific forward primer and a universal reverse primer (Wu *et al.*, 2007).
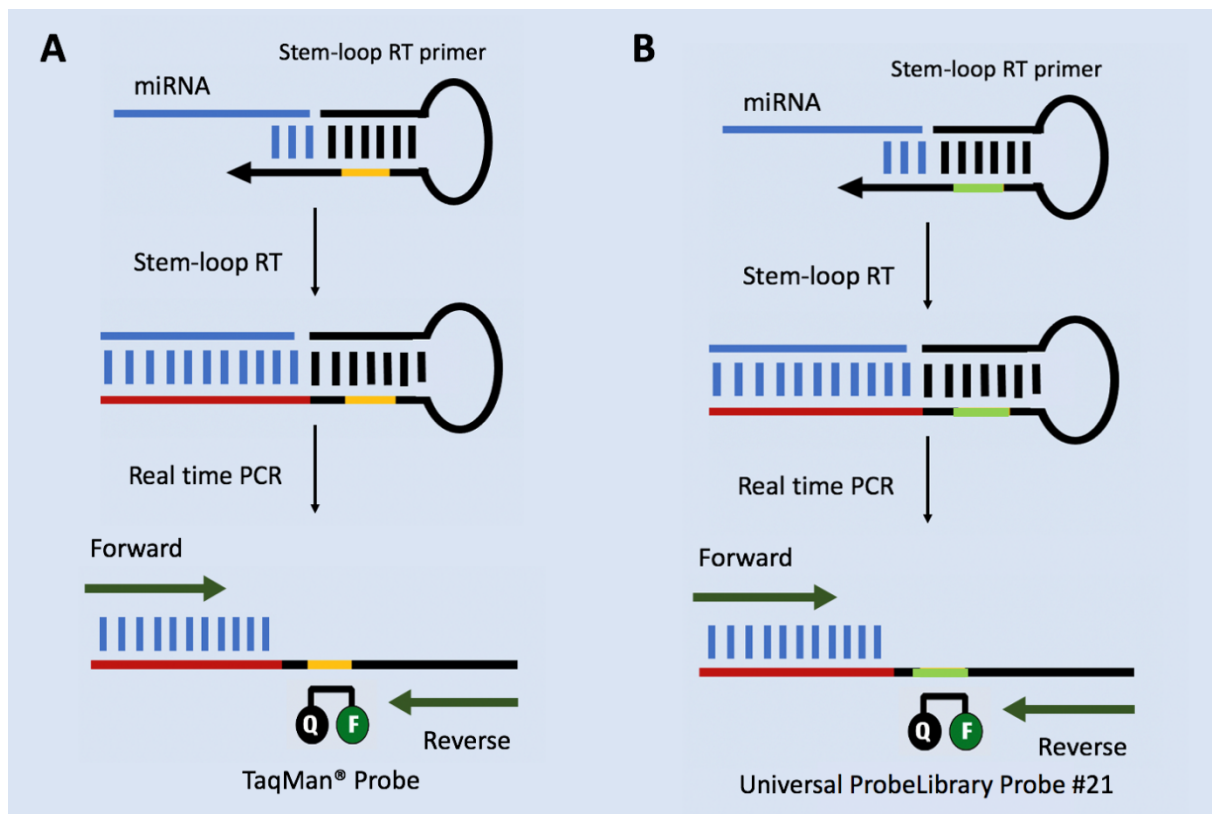
Figure 3.5: Real-time PCR miRNA assays.

MiRNA assays include two steps, an initial stem–loop RT and a subsequent real-time PCR. Stem–loop RT primers bind to the 3' portion of miRNA molecules, initiating reverse transcription of the miRNA. Highlighted in yellow is the TaqMan probe while the Universal Library Probe is highlighted in green. The RT product is quantified using PCR with a miRNA specific forward primer and the universal reverse primer. **(A)** TaqMan probe assay **(B)** Universal ProbeLibrary probe assay. Figure adapted from Wu *et al.* (2007).

3.2.1. Optimisation of RNA extraction

Accurate and reliable analysis of gene expression depends on the extraction of pure and high-quality RNA. There are two methods typically used for RNA extraction: commercially available silica spin column kits versus phenol-chloroform based extraction. Standard silica spin column kits typically exclude RNA under 200 nt and therefore would be unsuitable for studying miRNA expression (Rodríguez *et al.*, 2020). This is the case for the Spectrum Total

Plant RNA Kit (Sigma Aldrich) that is the standard method for RNA extraction in the Wellmer laboratory.

Phenol-chloroform extraction is a liquid-liquid extraction technique used to separate nucleic acids from proteins and lipids. This method utilises the fact that the phenol-chloroform mixture is immiscible with water. This results in two distinct phases forming. The lower (organic) phase and phase interface contain denatured proteins, while the less-dense upper (aqueous) phase contains nucleic acids. The phase extraction of nucleic acids is dependent on pH. A pH greater than 7 results in RNA and DNA resolving in the aqueous phase. However, an acidic pH results in DNA resolving in the organic phase, while RNA will remain in the aqueous phase. This allows for the aqueous phase containing the RNA to be removed and precipitated with alcohol (Chomczynski and Sacchi, 2006; Toni *et al.*, 2018)

The phenol-based reagent TRIzol was chosen for RNA extraction due to its accessibility, economic cost and the ability to extract miRNAs. One issue commonly associated with phenol-chloroform extractions is the presence of phenol, chloroform, guanidine and salt which can contaminate samples and effect the quantification of RNA on spectrophotometers as well as impacting downstream assays. To overcome this issue, RNA extraction was optimised following the method described by Toni *et al.* (2018). This method utilises an additional chloroform extraction step as well as several wash steps.

The phenol-chloroform extraction protocol from Toni *et al.* (2018) was compared to a traditional phenol-chloroform method which only has a single chloroform extraction and a single RNA wash step. RNA extraction was performed twice with two technical replicates. For interest's sake, it was also compared to RNA extracted from Spectrum Total RNA kit using two technical replicates.

The quality of the RNA was determined through the use of the Agilent TapeSation system. The TapeStation system is an automated electrophoresis solution for the sample quality control of DNA and RNA samples. This system utilises an RNA Integrity Number (RIN), which is a software algorithm that determines RNA quality and integrity. This comprehensive system removes any human interpretations of good RNA quality and integrity. It is calculated by the relative ratio of fast zone signal to 18S peak signal resulting in the RIN equivalent (RIN^e). RIN^e values range from 1 to 10; 10 being completely intact RNA, 1 being completely degraded. It is recommended to only use samples with a RIN^e of

6.5 and above. One caveat of this system is that it is optimized for mammalian RNA rather than plant RNA however it still stands as a measure for RNA integrity (Schroeder *et al.*, 2006).

The average RIN[e] scores for the RNA extracted through the various methods as well as the average concentration of the RNA can be seen in Table 3.3 and Figure 3.6. The results show that while the RNA concentration is lower using the method by Toni *et al.* (2018), the RIN score is much higher which indicates higher RNA integrity and quality. Interestingly, the quality of RNA is higher using the Toni *et al.* method than it is using the Spectrum Total RNA kit.

Table 3.3: Table comparing the quality and quantity of RNA extracted through different methods.

Higher RIN[e] scores indicate higher quality and integrity of RNA. Concentration and RIN score are the average of the two technical replicates for each method.

Method	RIN	Concentration
Traditional Phenol-chloroform Extraction	6.3	333 ng/ul
Toni *et al.* Phenol-chloroform Extraction	8.3	160 ng/ul
Spectrum Total RNA kit	6.7	345 ng/ul
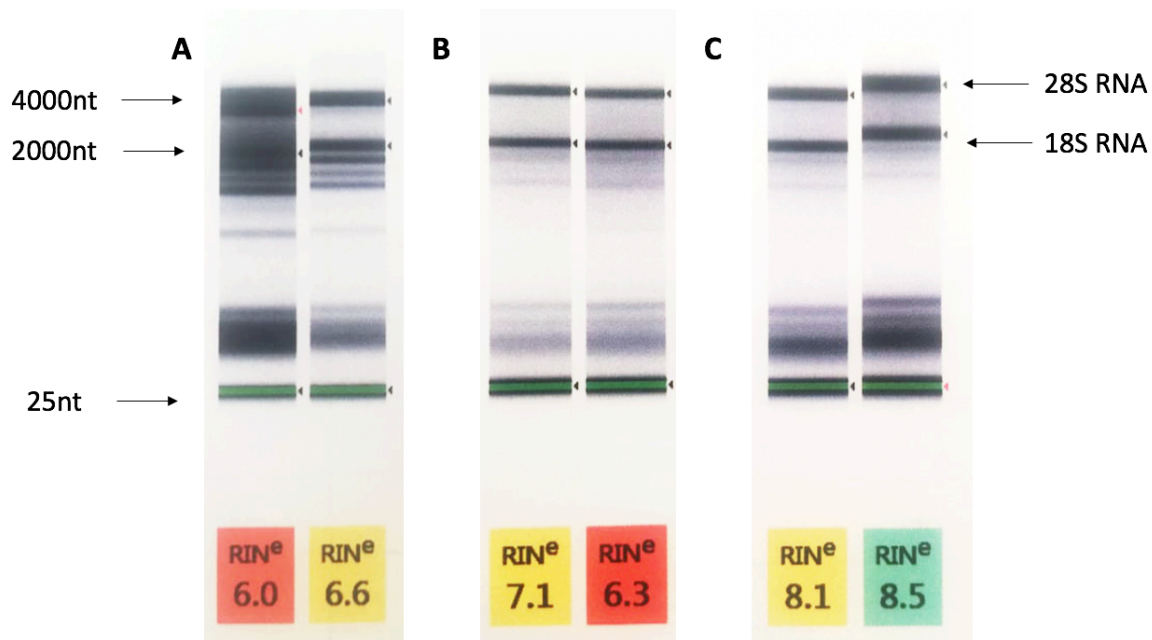
Figure 3.6: RNA analysis using the Agilent TapeStation system.

The gel image shows the separation profile of each sample along with the RIN score. RNA extraction was performed twice with two technical replicates for each sample. (**A**) Traditional Phenol Chloroform extraction. (**B**) Spectrum Total RNA kit. (**C**) Chloroform extraction after Toni *et al.* (2018). The electropherogram shows ribosomal RNA peaks of 28S and 18S as well as a ladder.

3.2.2. Reverse Transcription Optimisation

Pulsed RT reactions have been reported to provide better detection sensitivity when compared to non-pulsed reactions (Kikuchi *et al*., 2015). The logic behind this is that miRNA priming may be less efficient due to variations in sequence-dependant hybridisation of multiple targets. Therefore using a pulsed RT reaction of 60 cycles at 30°C for 30 seconds, 42°C for 30 seconds, and 50°C for 1 second provides more opportunities to transcribe all of the microRNA targets. This was investigated by comparing pulsed versus non-pulsed RT reactions using the same RNA sample and two technical replicates. Each reverse transcription reaction included a no template control (NTC) and a no reverse transcriptase control (NRT). The pulsed reactions resulted in a mean lower Ct (20.32) than the non-pulsed reactions (21.87). This is a three-fold change in gene expression. This indicates that there is

a significantly higher amount of the target miRNA when reverse transcribed with a pulsed method. Subsequently, the pulsed method was used to reverse transcribe miRNA. Neither of the NRC controls produced a detectable signal. NRT controls produced amplification curves after 37 cycles, more than 15 cycles with the same amount of RNA in the plus-RT reactions. Therefore, the background signal can be considered negligible.

3.2.3. Stem loop RT-qPCR with Universal Probe Library Optimisation

The stem-loop RT-qPCR method was combined with Universal ProbeLibrary (UPL) technology and investigated for its ability to reliably detect specific miRNAs. The dynamic range and sensitivity of the miRNA quantification scheme were first evaluated by comparing the results reported in the paper with replicate results produced in the laboratory (Wu *et al.*, 2007).

For this, the experimental conditions replicated those of the published results. This included the same primers, pulsed cDNA generation and identical LightCycler conditions. The assay itself consisted of 0.5 μM of each forward and reverse primer, 0.1 μM Universal ProbeLibrary Probe #21, 1x LightCycler® TaqMan® Master, and 1 μl of cDNA resulting in a final reaction volume of 20 μl. The amplification curves were generated with an initial denaturing step at 95°C for 10 minutes, followed by 45 cycles of 95°C for 5 seconds, 60°C for 10 seconds, and 72°C for 1 second. The only difference was the RNA used to generate cDNA. Wu *et al.* (2007) used total RNA isolated from shoots of 4-week-old Arabidopsis seedlings while RNA from FIS-AR AG-amiR^{DEX} flowers was used in Fig. 3.7B.

The results of this comparison can be seen in Fig. 3.7. The amplification curves for miR166 and miR156 reported in the paper can be seen in Fig. 3.7A and B. The replicate results can be seen in Figure 3.7B and D. The amplification curves for miR166 at different RNA amounts (from 20 ng to 20 pg total RNA) are similar to the published paper with a slightly later call of around 25 cycles (versus 21 cycles) for 20 ng of RNA. The greater amount of RNA (20 ng) results in an early peak call in both Figure 3.7A and B. The extra curves seen in Fig. 3.7B and D are due to technical replicates.

The miR156 expression data mirrors that of the results produced in the lab. However, the slope of the replicate results is slightly weaker in Figure 3.7D and the plateau of the curve is

not as pronounced. The weaker curve can be the result of the T_m value being too high resulting in less effective primer annealing. However, as the the T_m value used was identical to that published, this is unlikely the case. More than likely, there is some sample-specific PCR inhibition that slightly effects the efficiency of the reaction. Overall, the amplification curves are similar to those reported by Wu *et al.* (2007) indicating that this method is a reliable way of detecting miR166 and miR156 levels.

C.)

Amplification curves miR 156

Fluorescence (530 nm) vs Cycle number

D.)

Amplification Curves

Fluorescence (483-533) vs Cycles
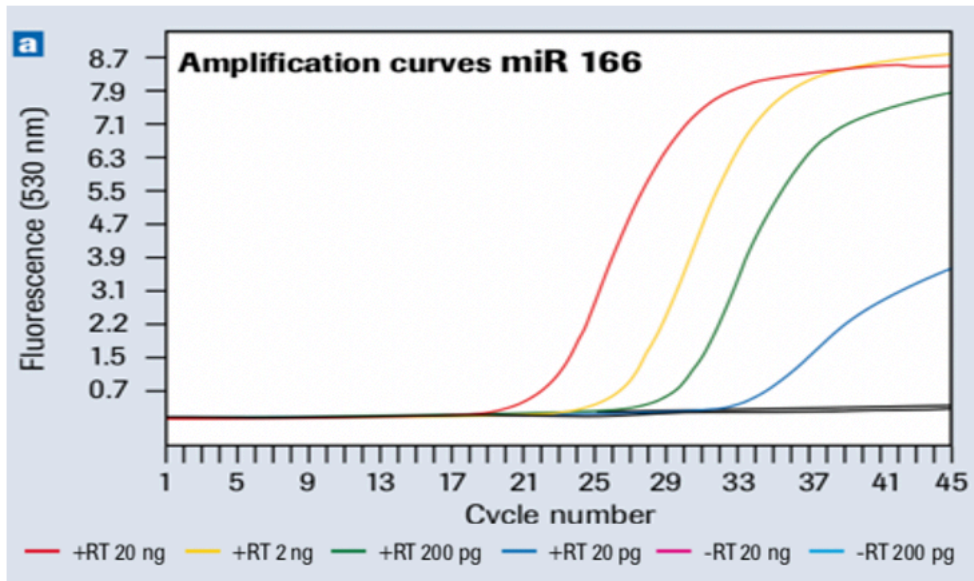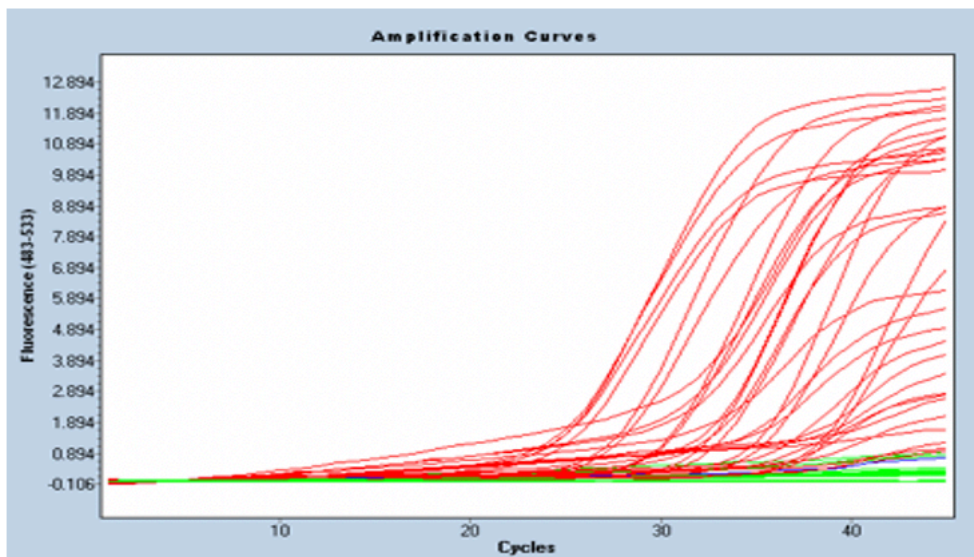
Figure 3.7: Replicating the amplification curves for miR166 and miR156.

Amplification curves were detected using Universal ProbeLibrary Probe #21 for (A) miR166 and (C) miR156 as reported by Wu et al. (2007). (B) Replicate results for miR166 and (D) miR156 produced in the Wellmer laboratory,

3.2.4. Reference genes and controls for the stem-loop RT-qPCR protocol

Relative quantification of data obtained from RT-qPCR is used to determine changes in gene expression across multiple samples or conditions after normalisation to an internal reference gene. Therefore, the accuracy of any RT-qPCR reaction relies on the availability of reliable reference genes. These reference genes need to maintain stable expression levels in different cell types, tissues and experimental conditions or treatments. Thus, this allows them to act as an endogenous control for normalisation of the data.

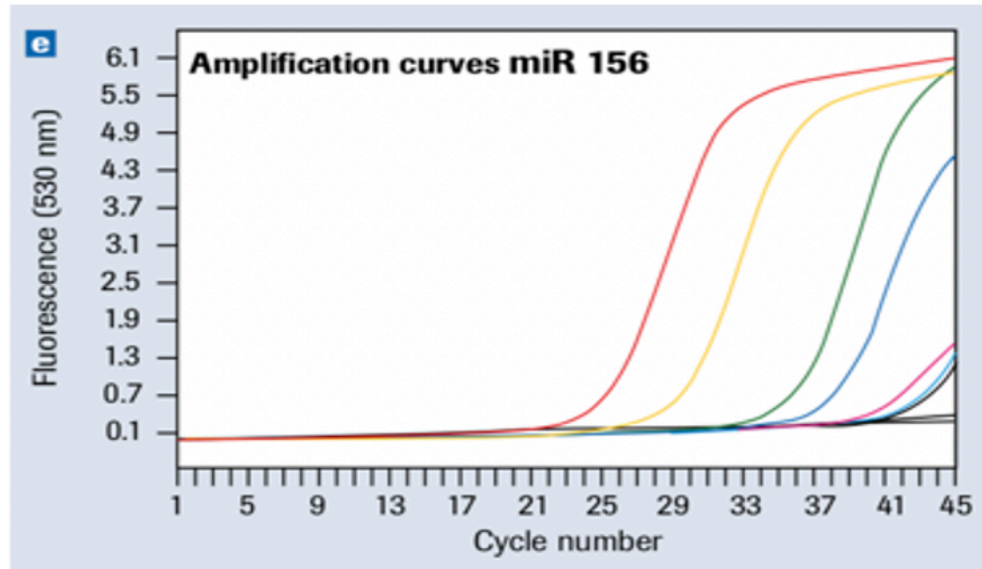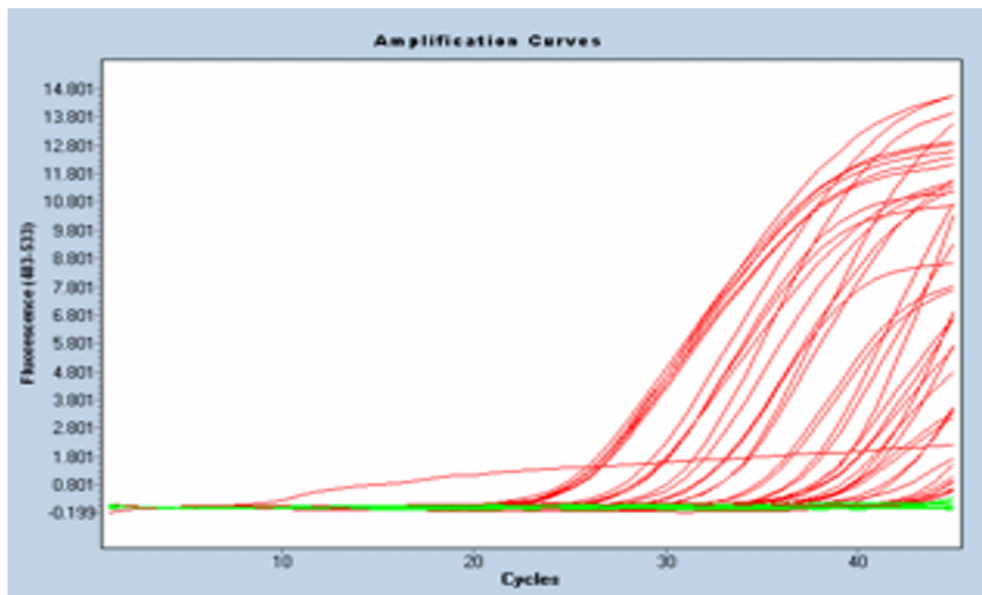Due to their extremely high expression, U6 snRNA, 5S rRNA/tRNA and ubiquitin genes are commonly used as reference genes for miRNA detection in Arabidopsis. In this study, six primer sets for U6 snRNA and *UBIQUITIN 10 (UBQ10)* were tested for their use as a reference gene. The primers were tested using RNA from four different tissue samples to ensure they have stable expression levels in different tissues.

The amplification curves for these reference genes resulted in a straight line rather than the expected sigmoidal curve. An example of this can be seen in Fig. 3.8 which is the amplification curve for a *UBQ10* primer set. As this may be indicative of a sample-specific PCR inhibition, the reaction was repeated with new starting materials however this still resulted in a straight slope rather than a sigmoidal curve. Additionally, the Cp values for these reference genes varied between RNA samples, with a range from 24 Cp to 32 Cp, indicating that they were not a reliable reference genes. None of the six primer sets for the U6 snRNA and UBQ10 resulted in a reliable reference gene that could be used to study miRNA relative expression.

One internal control that was identified in this study was a stem-loop primer designed for human miR122. This control consistently did not result in a detectable signal indicating that the stem-loop primers used in this study were specific to Arabidopsis.
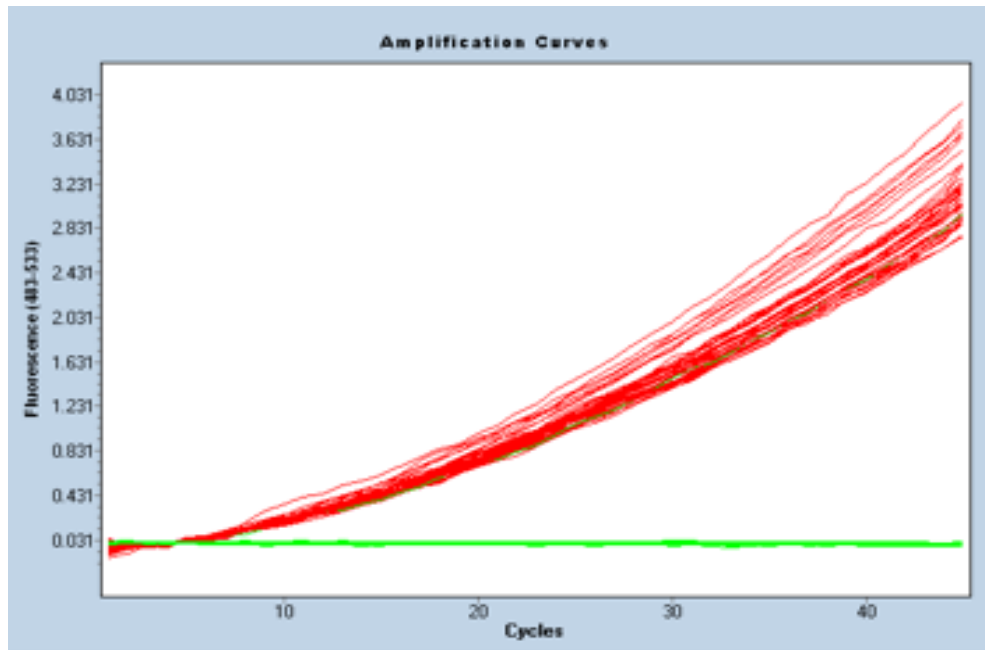
Figure 3.8: Amplification curve for a UBQ10 primer set. The amplification curves for UBQ10 resulted in a straight line rather than the expected sigmoidal curve.

3.2.5 Mir-X miRNA First-Strand Synthesis and Mir-X miRNA qRT-PCR TB Green Kit

The lack of a reliable reference gene in Section 3.2.4 hampered the progress on a reliable miRNA detection protocol. Therefore, the decision was made to use the Mir-X miRNA First-Strand Synthesis and Mir-X miRNA qRT-PCR TB Green Kit. This kit has been used to examine miRNA expression in leaf development and drought tolerance in Arabidopsis (Yang *et al.*, 2019; Okuma *et al.*, 2020). While it is not as cost effective as the stem-loop RT-qPCR protocol, it has been shown to have a reliable reference gene and has gone through extensive quality assurance.

The Mir-X miRNA First-Strand Synthesis Kit converts miRNA into cDNA. In a single-tube reaction, the miRNA are polyadenylated and reverse transcribed using poly(A) polymerase and the kit's SMART® MMLV Reverse Transcriptase. The TB Green Advantage® qPCR Premix and mRQ 3' Primer are then used in the RT-qPCR with each miRNA-specific primer. The primers used in this study can be seen in Appendix 5.2. The reference genes used were ACTIN2 and U6 snRNA.

This kit was used to examine the effects of *AG* perturbation on miRNA with fundamental roles in leaf polarity specification. To this end, RNA from the FIS-AR AG-amiR[DEX] line at stage 8 of flower development was used. The results shown in Figure 3.9 are the mean of three independent biological replicates, and two technical replicates for stage 8 of flower development. There is only one value for miR164 expression due to a limitation in reagents.

Figure 3.9 shows the results of *AG* perturbation on leaf organ polarity genes and miRNAs. *AG* is being consistently down-regulated as was seen in Figure 3.4. The perturbation of *AG* expression levels leads to the downregulation of *PHV* which was also seen in Figure 3.4C.

AG perturbation leads to the down-regulation of the majority of the miRNA genes tested. Specifically, the expression of miR160, miR165, miR166 and miR164 are all reduced. miR165 and miR166 are responsible for restricting the expression of the HD-ZIPIII genes to the adaxial side of the developing leaf. miR166 and its target *PHB* have been shown to regulate *SPL/NZZ* which controls microsporogenesis and developing the internal boundary of the anthers (Li *et al.*, 2019). Additionally, it has been shown that miR165/166 are expressed in early ovule primordia to restrict the *PHB* expression domain to promote integument formation (Hashimoto *et al.*, 2018). Furthermore, miR164 is involved in regulating petal number in Arabidopsis. miR164 regulates the expression of *CUC1* and *CUC2* genes which is necessary for floral organ boundary formation during floral meristem establishment. Reduction in *CUC1* and *CUC2* activity results in the formation of less petals while *mir164* loss of function mutants result in the formation of extra petals (Baker *et al.*, 2005). There is no literature to suggest that miR160 plays a role in floral organ development. There primary roles are in leaf development and embryogenesis. These results suggest that AG regulates miRNAs that function in floral reproductive organ development as well as leaf development.

One miRNA that is up-regulated in response to *AG* perturbation is miR159. Interestingly, miR159 is a key miRNA regulating the development of male reproductive organs by targeting MYB family genes. In Arabidopsis and rice, miR159 is expressed at high levels in anthers and its overexpression causes male sterility resulting from the failure of pollen release. Therefore, this result may indicate that AG regulates miR159 expression to achieve proper anther development. Plants that are mutant for *MIR159A* and *MIR159B* have curled leaves which highlights the role of miR159 in leaf development. However, the

standard deviations for miR159 expression are large and therefore, the results would have to be confirmed through additional experiments before any conclusions can be drawn.
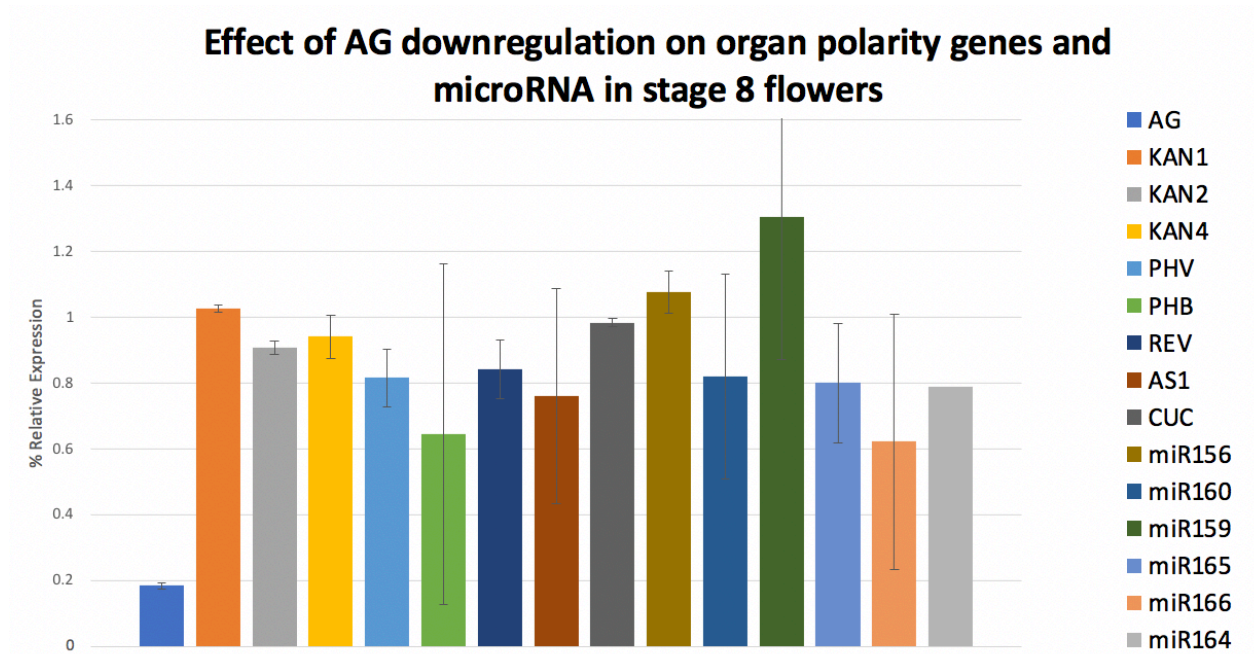
Figure 3.9: Effect of *AG* perturbation on the expression of organ polarity genes and miRNA genes in stage 8 flowers.

RT-qPCR results of the effect of *AG* downregulation on leaf polarity genes and miRNA genes in stage 8 flowers. Values are calculated using the Double Delta Cp analysis method. Values are the mean of three biological replicates. Two technical replicates were performed for each sample. Error bars represent standard deviations. There is only one value for miR164 due to a limitation in reagents.

The effect of *AG* down-regulation on organ polarity genes and miRNA genes was also examined in stage 3 flowers, and thus shortly after *AG* expression commences. The technical replicates were within 0.5 cycles of each other for the reference genes and genes tested however, there was a difference of 2 cycles between the mock and DEX-treated sample for the reference gene in one of the replicates. Ideally, reference genes should be invariable in

their expression levels which allows for the normalisation of data. Therefore, Fig. 3.12 only includes the mean values for two independent biological replicates.

There is a large downregulation in the levels of AS1 which was not seen in Fig. 3.4A to approximately 40% of their relative expression levels. AS1 expression levels were only down-regulated to 70% in Fig. 3.4A.

In regards to the miRNA genes, there is a large upregulation of miR159 expression with a small standard deviation (1.75 fold change). There is also a significant downregulation of miR165 expression levels to 50% their relative expression. This indicates that *AG* perturbation has a large effect on the expression of two of the microRNA genes in stage 3 of flower development.

Figure 3.10: Effect of *AG* down-regulation on the expression of organ polarity and miRNA genes in stage 8 flowers.
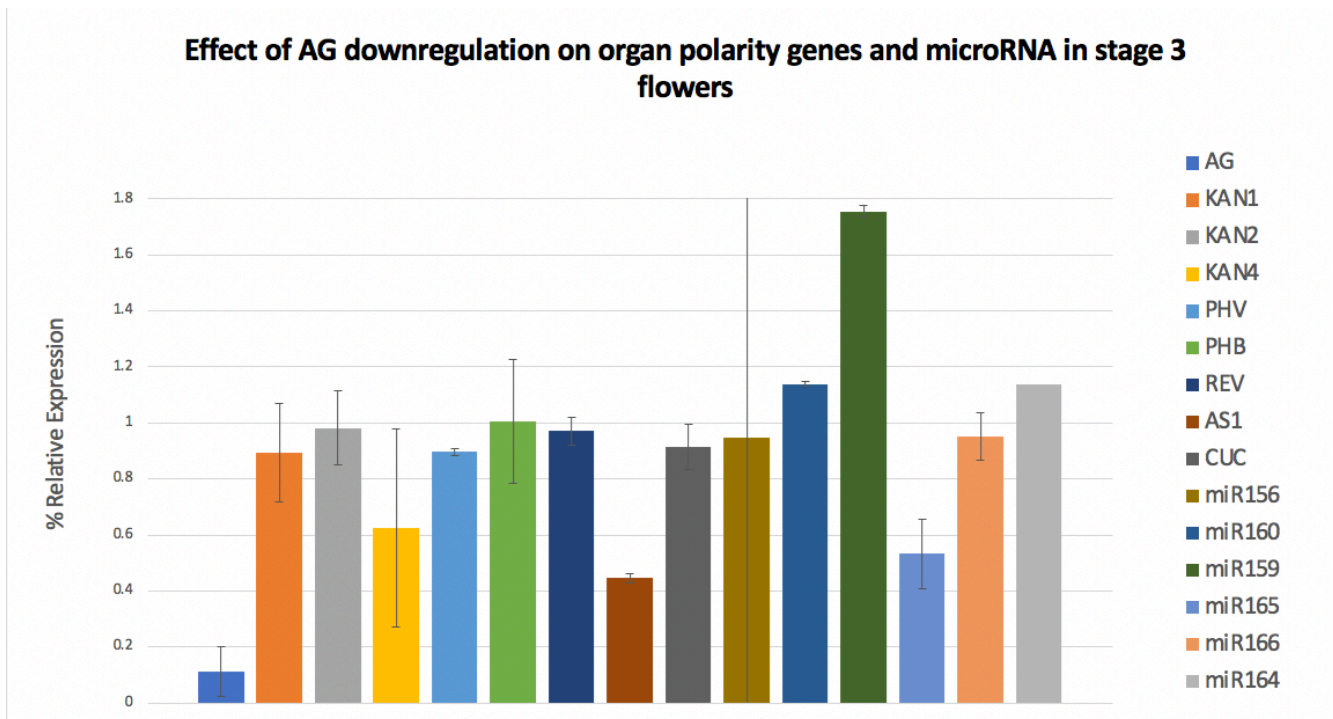
RT-qPCR results of the effect of *AG* downregulation on leaf polarity genes and miRNA genes in stage 3 flowers. Values are calculated using the Double Delta Cp analysis method. Values are the mean of two biological replicates. Two technical replicates were performed for each sample. Error bars represent standard deviations between the biological replicates. There is only one value for miR164 due to a limitation in reagents.

Chapter 4. Discussion

4.1.1 Interplay between AG and the floral homeotic factors

The first aim of this project was to investigate the interplay between the floral homeotic factor, *AG,* and the leaf polarity genes as previous evidence suggests these factors act together to control aspects of organ development.

The results outlined indicate that *AG* genetically interacts with the founding member of *KAN* gene family, *KAN1*. Together AG in flowers and KAN1 in leaves were shown to have a significant overlap in target genes (472) despite using very different tissue samples, namely early-stage flowers in the case of AG and rossette leaves in the case of KAN1. Microarray, RNA-seq and ChIP-seq data for AG as well as ChIP-seq data for KAN1 were compared. The data indicates that there is binding evidence with several genes involved in leaf organ polarity specification. Of the genes bound by AG, the majority is not differentially expressed when *AG* expression is altered. This could indicate that they are not directly regulated by *AG*. One point to note is that AG does not seem to directly bind to *KAN1* as evidenced by the ChIP-seq data. As this ChIP-seq was only preformed at one stage of flower development, it is possible that the interaction between AG and *KAN1* was missed. Otherwise, it can be presumed that another regulator activates *KAN1* in flowers.

Biological processes that were under- or over-represented in the overlap between the ChIP-seq data sets were identified by comparing the occurrence of GO terms within the lists of target genes to their genome-wide distribution using a two-sided Fisher's exact test. The GO terms for the overlap between the KAN1 and AG ChIP-seq datasets include '*Response to continuous far red light stimulus', 'Sucrose transport*', '*Radial pattern formation', 'Shoot formation*', '*Plant organ development*' and *'Brassinosteroid mediated signalling pathway.'*

There was a 28 fold enrichment for the GO term 'Sucrose transport' between the AG and KAN1 datasets. In growing plants, photosynthates (including sucrose) are produced in leaves by photosynthesis and are transported to sites of active growth which include flowers, fruits and seeds (Durand *et al.*, 2018). Recent evidence suggests that reproductive tissues not only require sucrose from leaves but are photosynthetically active and therefore produce sucrose themselves (Brazel and Ó'Maoileídigh, 2019). A closer examination of the AG regulated genes reveals that many of them have known roles in photosynthesis (O'Maoileidigh *et al.*, 2013). AG, therefore, may play a role in regulating sucrose transport in reproductive organs in flowers. The role of photosynthesis in the reproductive organs is a burgeoning field of research and provides further credence to the idea that floral organs are modified leaves. Additionally, KAN1 was previously shown to negatively regulate sucrose transport in leaves. (Xie *et al.*, 2015)*.* This indicates that KAN1 and AG regulate common target genes involved in sucrose transport in the leaf and flower, respectively.

Similarly, KAN1 and AG regulate common target genes involved in the brassinosteroid mediated signalling pathway as there was a 12 fold enrichment. Brassinosteroids are known to play an important role in gynoecium development. Brassinosteroid genes such as *BR-ENHANCED EXPRESSION* 1 (*BEE1*), *BEE2* and *BEE3* are involved in developing the transmitting tract in developing gynoecia development (Crawford and Yanofsky, 2011). Moreover, brassinosteroid-related mutants, de-etiolated2 and dwarf1, result in the development of small leaf size indicating their role in leaf development (Nakaya *et al.*, 2002).

A GO analysis for the 2,769 genes identified in the KAN1 ChIP-seq dataset revealed genes with enrichment in flower development and shoot/leaf patterning. Similarly, a GO analysis for the 1,487 genes in the AG ChIP-seq dataset shows an over-representation in flower development and patterning categories. This similarity is more than likely due to their natures as regulators of development and polarity. One caveat to this is this is the ChIP-seq data sets are at different stages of plant development.

To fully examine if *AG* and *KAN1* are acting together to control aspects of flower development, a KAN1 ChIP-seq would have to be performed in flowers at the same stage and conditions as *AG*. This would allow us to identify KAN1 target genes in flowers. To this end, a ChIP-seq using the KAN-GFP line crossed into the FIS could be conducted.

Additionally, RNA-seq could be performed to examine the effects that the specific activation or down-regulation of *KAN1* has on gene expression in flowers. This could be performed with the p35S::KAN-GR line used by Merelo *et al.* (2013). This line mediates ubiquitous activity of KAN1 upon addition of DEX. Otherwise, a KAN1-amiRNA line could be created to allow for the specific down-regulation of *KAN1* in flowers. This would allow for normal plant development until the required experimental stage. Ideally, both of these lines would be crossed into the FIS to allow for synchronisation of flower development. The results from these two lines of experiments could then be compared to the similar studies discussed in Section 3.1.1.

4.1.2. The Response of Leaf Polarity Genes to AG Perturbation

In Section 3.2.3, the effects of the specific downregulation of *AG* on leaf polarity genes was examined in various stages of floral development. The results of which resulted in a relatively small transcriptional change to the majority of the organ polarity genes tested. These results correspond with the data from Dr. Bennett Thomson (Fig. 3.1) which highlights the minor changes in gene expression levels of the leaf polarity genes to *AG* perturbation.

The largest down-regulation was of *PHV* in stage 5 and 8 of floral development to approximately 65%. This correlates with previous work shown in Figure 3.2B that indicates a transcriptional response of *PHV* to *AG* perturbation in microarray experiments. To reiterate, *PHV* is a member of the HD-ZIPIII class of genes that specifies adaxial polarity in leaves. It works redundantly with *REV* and *PHB* which makes it interesting that they were not affected by *AG* perturbation more. Experimentally, *PHV* has been shown to work cooperatively with *PHB* and *CORONA* to repress *WUS* expression in the chalaza of the ovule and this repression is key for proper ovule development (Yamada *et al.*, 2016). *AG* may be facilitating this interaction. It is interesting to note that this downregulation occurs at stage 5 of flower development while ovules do not form till stage 11 of flower development (Smyth, 1990). This indicates that PHV may be playing an additional role in reproductive organ development prior to proper ovule development. To further investigate this interaction, confocal imaging could be used to identify the expression patterns of *PHV* in the gynoecium and to investigate if these expression patterns change as a result of *AG* perturbation. Additionally, a *phv* loss of function mutant could be crossed with the AG-

amiRNA[DEX] line to examine if there is a phenotypic effect when *AG* expression is downregulated.

One way to examine if *AG* has a functional effect on the leaf polarity genes, such as *PHV*, would be to locate and mutate CArG-box sequences in the leaf polarity genes. CArG-box sequences have been well defined and characterised which allows for their identification (Aerts *et al.*, 2018). To show that these sites are indeed functional, they could be mutated through CRISPR/Cas9 genome editing. The resulting lines could then be examined for phenotypic abnormalities which would be expected if the regulation of *KAN* genes by AG is indeed functionally important.

The lack of a larger transcriptional response of the leaf organ polarity genes to *AG* perturbation could be explained by several lines of reasoning. Firstly, as the evidence suggests that *AG* and *KAN1* work in concert to control gene expression, it is likely that these genes work redundantly to regulate organ polarity in the reproductive floral organs. Therefore the downregulation of just *AG* may not have a large effect on the polarity genes as they are also regulated by *KAN1*.

To investigate this hypothesis further, the FIS-AR AG-amiRNA[DEX] line could be crossed into the *kan1-1* mutant line. This would allow us to investigate the extent of the redundancy between these genes by looking at specific *AG* perturbation in the *kan1-1* mutant background.

Additionally, AG could be regulating these leaf polarity genes indirectly through other targets or via microRNAs. One potential target is *TARGET OF EAT1 (TOE1)*. A recent paper examined the heteroblastic development of trichomes in Arabidopsis. Heteroblasty refers to the development of organs in an age-dependant manner. In this case, the production of abaxial trichomes is a heteroblastic mark for the juvenile to adult transition of the plant. This paper showed that abaxial trichomes are prevented from developing on the abaxial side of the leaf in juvenile development through a repressive complex of *KAN1-TOE1* (Wang *et al.*, 2019). Trichomes are formed in leaves through an activator complex consisting of *GLABRA1 (GL1), GLABRA3 (GL3)* and *TRANSPARENT TESTA GLABRA 1 (TTG1)* (Bernhardt et al., 2005; Pattanaik et al., 2014). This complex initiates the expression of *GLABARA2,* which results in the development of a trichome cell. In the juvenile phase a the abaxial side of the leaf, the *KAN1-TOE1* complex represses this activator complex through

chromatin looping. As the plants age, this complex no longer exists resulting in trichomes on the abaxial side (Wang et al., 2019). ChIP-seq results for AG indicate binding evidence for *AG* and *TOE1* (O'Maoileidigh *et al.*, 2013). As *TOE1* directly binds *KAN1, AG* could be regulating the leaf polarity genes indirectly through *TOE1*. One way to investigate this further would be to repeat the RT-qPCR experiments from Section 3.1.3. to investigate the effect of *AG* perturbation on *TOE1* expression in flowers.

Furthermore, in the recent paper by the Wellmer laboratory, it was shown that parts of the genetic program for leaf development remains active during flower formation however this pathway has been partially rewired by the floral homeotic proteins (Ó'Maoiléidigh *et al.*, 2018). If this hypothesis is applied to this research, it is feasible that *AG* regulates leaf polarity genes by rewiring the pre-existing leaf development program which relies heavily on microRNA regulation. To investigate this further, a reliable microRNA detection protocol would allow us to investigate if *AG* perturbation has an effect on the microRNAs involved in abaxial/adaxial polarity in leaves. This will be discussed in Section 4.3. Furthermore, the ChIP-seq techniques in *AG* would have to be redone as the RNA extraction protocol used in these methods excludes small RNAs. Therefore, mature miRNAs were not detected.

Moreover, the lack of a large effect on the organ polarity genes when *AG* is down-regulated could be due to a timing issue. The interaction between *AG* and these genes could be transient and missed in these experimental conditions. We may see a larger effect if the *AG* was down-regulated for longer. Previous work by Dr. Bennett Thomson showed sustained down-regulation of *AG* for several days after a single application of DEX (Thomson, 2017). These experiments could be repeated allowing for sustained *AG* down-regulation.

Overall, the combined results of the genetic, genomic and molecular analyses suggest that the activities of the floral homeotic protein, AG, are superimposed onto the leaf polarity network. AG appears to regulate leaf polarity by targeting members of the KAN family. However, *AG* perturbation had only weak effects on the expression of these genes implying that additional pathways might contribute to this process.

4.3.1. Optimisation of RNA extraction and reverse transcription

The second aim of this project was to establish a reliable microRNA detection protocol. To this end, RNA extraction was optimised to ensure that mature microRNAs were being detected and that the RNA was of an extremely high quality. The results show that the Toni *et al.* (2018) phenol-chloroform extraction method yields the highest quality RNA with an average RIN^e score of 8.5. Therefore, this should be the primary method of RNA extraction in the lab. One caveat to this procedure is that it is slightly more time consuming particularly in cases where there are a lot of samples.

Pulsed RT reactions were also shown to provide better detection sensitivity in comparison to non-pulsed reactions. When comparing pulsed versus non-pulsed RT reactions using the same RNA sample and two technical replicates, the pulsed reactions lead to a lower Ct (20.32) than the non-pulsed reactions (21.87). This indicates that the miRNA are being more reverse transcribed with a pulsed method.

4.3.2. Stem-Loop RT-qPCR with Universal Probe Library Optimisation

The stem-loop RT-qPCR with Universal Probe Library Optimisation was examined for its ability to reliably detect specific miRNA. This was first evaluated with its ability to detect the microRNA described in the paper, namely miR166 and miR156. Through replicating the results from the paper, it was shown that the stem-loop RT-qPCR technique could reliably detect miR156 and miR166 expression. The other miRNA detected in the paper were miR159 and miR167.

One interesting thing to note is that the levels of miR166 and miR156 were largely identical between the paper and the replicate results despite using RNA from different tissues. Wu et al. (2007) used total RNA isolated from shoots of 4-week-old *Arabidopsis* seedlings while RNA from FIS-AR AGamiR^{DEX} was used in Figure 3.7b and d.

One major issue with the Stem loop RT-qPCR method was the inability to identify a reliable reference gene. In this study, six primer sets for U6 snRNA and *UBIQUITIN 10 (UBQ10)* were tested for their use as a reference gene. The primers were tested using RNA from four different tissue samples to ensure their reliability across different tissue types.

As evidenced in Figure 3.8, the amplification curve for the reference gene *UBQ10* resulted in a straight line rather than the expected sigmoidal curve. This result occurred with each of the primer sets tested. As this may be indicative of a sample-specific inhibitor, the experiments were repeated with new starting material. This still resulted in a straight slope and not a sigmoidal curve. One explanation for this could be a Tm value that is too high. This can result in primers that are unable to bind with their priming sites resulting in a poor per-cycle efficiency. The Tm used for these experiments was 60°C as this value allowed for the efficient amplification of miR166 and miR156. The Tm value of the cycling conditions could be reduced to see if this allows for sigmoidal amplification curves.

Due to the lack of a reliable reference gene, the decision was made to use the Mir-X miRNA First-Strand Synthesis and Mir-X miRNA qRT-PCR TB Green Kit. This kit allowed for the effect of *AG* perturbation on miRNA genes to be determined. The microRNA genes chosen for examination were miR156, miR160, miR159, miR165, miR166, and miR164. All of these genes have known roles in specifying the abaxial/adaxial polarity of leaves. As evidenced in Figure 3.4, *AG* perturbation does not have a large effect on the expression of leaf polarity genes. One reason for this may be that *AG* works indirectly through other targets such as microRNA genes.

From Figures 3.9 and 3.10, it is clear that *AG* perturbation has a larger effect on the miRNA genes than the leaf organ polarity genes tested. For example, *AG* perturbation leads to the downregulation of miR160, miR165, miR166 and miR164 in stage 8 flowers and miR165 in stage 3 flowers. miR165 and miR166 have been shown to regulate microsporogenesis as well as anther boundary and ovule development.

The expression levels of miR159 were upregulated in stage 3 and stage 8 flower development. miR159 is a key miRNA regulating the development of male reproductive organs by targeting MYB family genes. In *Arabidopsis* and rice, miR159 is expressed at high levels in anthers and its overexpression causes male sterility resulting from the failure of pollen release. Therefore, this may indicate that *AG* expression regulates miR159 expression for proper anther development.

From these results, it appears that *AG* regulates the organ polarity genes indirectly through miRNA gene expression. One future experiment of interest would be to examine how *AG*

perturbation effects ta-siRNA expression which is required to restrict *ETT*, *ARF2*, and *ARF4* expression to the abaxial side. Additionally, it would be interesting to cross the AG-amiRNA^{DEX} line into a *miR159* mutant to examine any phenotypic changes when AG expression is downregulated. Alternatively, the *miR159* gene sequence could be examined for a CARG box which is where AG binds. This CARG box could be mutated to see the effect of *AG* regulation on flower formation.

4.4. Future Work and Conclusions

This project had two broad aims. The first was to investigate the knowledge gap of genes that are known to control the shape and the polarity of leaves but are also active during floral organ development. Previous evidence suggests that the interplay of the organ polarity regulators and the floral homeotic transcription factors act together to control aspects of floral organ development. To this end, *AG* is used a proxy to examine the interplay between the floral homeotic factors and the genes governing organ polarity. From the evidence in this research, it appears as though *AG* works in concert with *KAN1* to control aspects of floral development.

Our knowledge of the interaction between *AG* and the organ polarity genes could be expanded through several lines of experiments. The first being the examination of the role of *KAN1* in flowers. This could be implemented through a KAN1 ChIP-seq. This would allow us to identify *KAN1* target genes in flowers. The results of this ChIP-seq could then be compared to the AG-ChIP to better understand their interaction. Additionally, RNA-seq could be performed to examine the effects that the specific activation or down-regulation of *KAN1* has on gene expression in flowers. Finally, the interaction between the other floral homeotic factors and the leaf organ polarity genes could be investigated. This would provide further evidence to the idea that floral organs are modified leaves and that the floral homeotic factors are superimposed on the leaf development program.

As the floral homeotic factors work in a combinatorial manner with other transcription factors and microRNAs to specify organ identities in flowers, the second aim was to

establish a reliable and effective microRNA detection protocol. Several aspects of this process were optimised such as RNA extraction and pulsed reverse transcription, however a reliable reference gene was not identified. Therefore, a different microRNA detection method was used. This protocol allowed us to investigate the interplay between the floral homeotic factors and miRNA involved in leaf polarity specification. The results indicate that *AG* perturbation effects the gene expression of miRNAs that have known roles in leaf and flower development. Furthermore, *AG* perturbation has a larger effect on miRNA expression than on the leaf polarity genes. This may indicate that the floral homeotic factors regulate the shaping of floral organs through miRNA regulation. Contextually this may be relevant in the context of floral evolution and that differences in their interactions may explain the astounding variations in floral morphologies found among different angiosperms.

5. Appendix

Table 5.1. RT-qPCR primer sequences used.

Primer	Sequence (5' to 3')
DM242	AAGCGGTTGTGGAGAACATGATACG
DM243	TGGAGAGCTTGATTTGCGAAATACCG
DM534	ACCAGATTCTTCGTGCAAAGATAGCTG
DM535	AAGCTGCTCGTAGTTAGATCCTCCTG
DM357	ACTTCTGGAAACGAACCGCTTCAG
DM358	CGGATGAAACGGATCGTAGCCATC
KH1	TCATCGACGGATCAAAGGGC
KH2	ATGGCCATGTCTCTCGTGAAG
KH9	CAGCAGCTTCGTCAGGACA
KH10	CCATGCAAACGTGCTTCTCC
KH21	ACCCAAAGAGCTTCATGGTCATC
KH22	TCACTGGAGGGTTCCGCATA
KH27	GTTGCAGAATGTTCCACCCCT
KH28	GTTCGAGTGTCTGTGCGAGA
KH35	GTTGCTTCAGAACGTTCCACC
KH36	AGCATAAGCATCCACGCCAT

KH45	ATGCCATCCTGTGTTGCTCA
KH46	GCAAGCAAGCAAATCCCTGT
KH47	TCGTGTACGTCGTCTGGTTT
KH48	TCTCACCATCCTTCTTCATCAAATG
KH53	CTCCGCTAAGGATGAATGGGT
KH54	CAATTGCAGAACCGGCAGAG

Table 5.2. MicroRNA primer sequences

Primer	Sequence (5' to 3')
KH32_Universal	GTGCAGGGTCCGAGGT
KH33_miRNA156a_RT	GTTGGCTCTGGTGCAGGGTCCGAGGTATTCGCACCAG AGCCAACGTGCTC
KH34_miRNA156a_F	GCGGCGGTGACAGAAGAGAGT
KH35_miRNA166a_RT	GTTGGCTCTGGTGCAGGGTCCGAGGTATTCGCACCAG AGCCAACGGGGAA
KH36_miRNA166a_F	TCGCGTGAAGCTGCCAGCAT
KH37_human_miR122_RT	GTTGGCTCTGGTGCAGGGTCCGAGGTATTCGCACCAG AGCCAACCAAACA
KH38_human_miR122_F	GCG CCG TGG AGT GTG ACA
KH39_AG_amiRNA_RT	GTTGGCTCTGGTGCAGGGTCCGAGGTATTCGCACCAG AGCCAACGCTGAT
KH40_AG_amiRNA_F	GCC CGC TTT ATC GTT ATG CAA ATC AGC
KH41_miRNA165_RT	GTTGGCTCTGGTGCAGGGTCCGAGGTATTCGCACCAG AGCCAACGGGGAT
KH42_miRNA165_F	TCC GAT GAA GCC TGG TCC GA
KH43_U6ref_RT	GTTGGCTCTGGTGCAGGGTCCGAGGTATTCGCACCAG AGCCAACTTTGCA

KH44_U6ref_F	CGT GTG GGG GAC ATC CGA TAA
KH45_U6ref2_RT	GTTGGCTCTGGTGCAGGGTCCGAGGTATTCGCACCAG AGCCAACCCAAAT
KH46_UBI10_1_RT	GTTGGCTCTGGTGCAGGGTCCGAGGTATTCGCACCAG AGCCAACTTTTAT
KH47_UBI10_1_F	CGC GGG GTT TAT CAA CTC AAA GC
KH48_UBI10_2_RT	GTTGGCTCTGGTGCAGGGTCCGAGGTATTCGCACCAG AGCCAACAGAGGG
KH49_UBI10_2_F	CGC ACT TTG GTC CTC AGG CTC
KH50_UBI10_3_RT	GTTGGCTCTGGTGCAGGGTCCGAGGTATTCGCACCAG AGCCAACGTGTTG
KH50_UBI10_3_F	GATCCAGGATAAGGAAG
KH51_miRNA159a_RT	GTTGGCTCTGGTGCAGGGTCCGAGGTATTCGCACCAG AGCCAACTAGAGC
KH52_miRNA159a_F	CGGCGGTTTGGATTGAAGGGA
KH53_miRNA166a_F	TTCCTTGATTGAGCCGCGCC
KH54_miRNA165a_RT	GTTGGCTCTGGTGCAGGGTCCGAGGTATTCGCACCAG AGCCAACCCTCGA
KH55_miRNA165a_F	GCG CCT GGA ATG TTG TCT GG
KH56_miRNA166b_RT	GTTGGCTCTGGTGCAGGGTCCGAGGTATTCGCACCAG AGCCAACCTCGAG
KH57_miRNA166b_F	CGC ACT GGA CTG TTG TCT GGC
KH58_U6ref_RT	GTTGGCTCTGGTGCAGGGTCCGAGGTATTCGCACCAG AGCCAACTGCAAA
KH59_U6ref_F1	ACT AAC GCA TGG CCC CTG C
KH60_U6ref_F2	GCG ACG CAC GCA TAA ATC GAG
KH61_miR156_F	GCTGACAGAAGAGAGTGAGCAC
KH62_miR160_F	TGCCTGGCTCCCTGTATGC
KH63_miR159_F	TTTGGATTGAAGGGAGCTCTA
KH64_miR165_F	TCGGACCAGGCTTCATCCC

KH65_miR166_F	AGCAGGGCACGTGCAAAA

6. References

Aerts, N. *et al.* (2018) 'Comparative analysis of binding patterns of MADS-domain proteins in Arabidopsis thaliana', *BMC Plant Biology*. BMC Plant Biology, 18(1), pp. 1–16. doi: 10.1186/s12870-018-1348-8.

Allen, E. *et al.* (2005) 'microRNA-directed phasing during trans-acting siRNA biogenesis in plants', *Cell*, 121(2), pp. 207–221. doi: 10.1016/j.cell.2005.04.004.

Alvarez-Buylla, E. R. *et al.* (2010) 'Flower Development', *The Arabidopsis Book*, 8(8), p. e0127. doi: 10.1199/tab.0127.

Aukerman, M. J. and Sakai, H. (2004) 'Erratum: Regulation of Flowering Time and Floral Organ Identity by a MicroRNA and Its Apetala2-Like Target Genes (Plant Cell (2003) 15 (2730-2741))', *Plant Cell*, 16(2), p. 555. doi: 10.1105/tpc.cor238.

Bar, M. and Ori, N. (2014) 'Leaf development and morphogenesis', *Development (Cambridge)*, 141(22), pp. 4219–4230. doi: 10.1242/dev.106195.

Borges, F. and Martienssen, R. A. (2015) 'The expanding world of small RNAs in plants', *Nature Reviews Molecular Cell Biology*. Nature Publishing Group, 16(12), pp. 727–741. doi: 10.1038/nrm4085.

Bowman, J. L. (1989) 'Genes Directing Flower Development in Arabidopsis', *The Plant Cell Online*, 1(1), pp. 37–52. doi: 10.1105/tpc.1.1.37.

Bowman, J. L., Smyth, D. R. and Meyerowitz, E. M. (1991) 'Genetic interactions among floral homeotic genes of Arabidopsis.', *Development*, 112(1), pp. 1–20. doi: 10.1242/dev.025148.

Bowman, J. L., Smyth, D. R. and Meyerowitz, E. M. (2012) 'The ABC model of flower development: Then and now', *Development (Cambridge)*, 139(22), pp. 4095–4098. doi: 10.1242/dev.083972.

Brazel, A. J. and Ó'Maoileídigh, D. S. (2019) 'Photosynthetic activity of reproductive organs', *Journal of Experimental Botany*, 70(6), pp. 1737–1753. doi: 10.1093/jxb/erz033.

Caggiano, M. P. *et al.* (2017) 'Cell type boundaries organize plant development', *eLife*, 6, pp. 1–32. doi: 10.7554/eLife.27421.

Carles, C. C. and Fletcher, J. C. (2003) 'Shoot apical meristem maintenance: The art of a dynamic balance', *Trends in Plant Science*, 8(8), pp. 394–401. doi: 10.1016/S1360-1385(03)00164-X.

Causier, B., Schwarz-Sommer, Z. and Davies, B. (2010) 'Floral organ identity: 20 years of ABCs', *Seminars in Cell and Developmental Biology*. Elsevier Ltd, 21(1), pp. 73–79. doi: 10.1016/j.semcdb.2009.10.005.

Chang, W. *et al.* (2020) 'Same Actor in Different Stages: Genes in Shoot Apical Meristem Maintenance and Floral Meristem Determinacy in Arabidopsis', *Frontiers in Ecology and Evolution*, 8(April), pp. 1–12. doi: 10.3389/fevo.2020.00089.

Chen, C. *et al.* (2005) 'Real-time quantification of microRNAs by stem-loop RT-PCR', *Nucleic Acids Research*, 33(20), pp. 1–9. doi: 10.1093/nar/gni178.

Chen, D. *et al.* (2018) 'Architecture of gene regulatory networks controlling flower development in Arabidopsis thaliana', *Nature Communications*. Springer US, 9(1), pp. 1–13. doi: 10.1038/s41467-018-06772-3.

Chitwood, D. H. *et al.* (2007) 'Establishing leaf polarity: The role of small RNAs and positional signals in the shoot apex', *Development*, 134(5), pp. 813–823. doi: 10.1242/dev.000497.

Chomczynski, P. and Sacchi, N. (2006) 'The single-step method of RNA isolation by acid guanidinium thiocyanate-phenol-chloroform extraction: Twenty-something years on', *Nature Protocols*, 1(2), pp. 581–585. doi: 10.1038/nprot.2006.83.

Chugh, P. and Dittmer, D. P. (2012) 'Potential pitfalls in microRNA profiling', *Wiley*

Interdisciplinary Reviews: RNA, 3(5), pp. 601–616. doi: 10.1002/wrna.1120.

Coen, E. S. and Meyerowitz, E. M. (1991). The war of the whorls: genetic interactions controlling flower development. *Nature* 353, 31-37.

Colombo, L., Franken, J., Koetje, E., van Went, J., Dons, H. J. M., Angenent, G. C., and van Tunen, A. J. (1995). The petunia MADS box gene FBP11 determines ovule identity. *Plant Cell* 7: 1859–1868

Crawford, B. C. W. and Yanofsky, M. F. (2011) 'Half filled promotes reproductive tract development and fertilization efficiency in Arabidopsis thaliana', *Development*, 138(14), pp. 2999–3009. doi: 10.1242/dev.067793.

Czechowski, T., Stitt, M., Altmann,T., Udvardi, M.K., and Scheible, W.R. (2005). Genome-wide identification and testing of superior reference genes for transcript normalization in Arabidopsis. *Plant Physiol*. 139: 5–17.

Darwin, C., (1859). The origin of species and The descent of man, New York (The Modern Library).

Darwin, C., (2010). The Works of Charles Darwin, Volume 25: The Effects of Cross and Self Fertilization in the Vegetable Kingdom. *NYU Press*.

Denay, G. *et al.* (2017) 'A flower is born: an update on Arabidopsis floral meristem formation', *Current Opinion in Plant Biology*, 35(Figure 1), pp. 15–22. doi: 10.1016/j.pbi.2016.09.003.

Dilcher, D. (2000) 'Toward a new synthesis: Major evolutionary trends in the angiosperm fossil record', *Proceedings of the National Academy of Sciences of the United States of America*, 97(13), pp. 7030–7036. doi: 10.1073/pnas.97.13.7030.

Ditta G, Pinyopich A, Robles P, Pelaz S, Yanofsky MF. (2004). The SEP4 gene of Arabidopsis thaliana functions in floral organ and meristem identity. *Current Biology* 14, 1935–1940

Dong, Z., Han, M. H. and Fedoroff, N. (2008) 'The RNA-binding proteins HYL1 and SE promote accurate in vitro processing of pri-miRNA by DCL1', *Proceedings of the National Academy of Sciences of the United States of America*, 105(29), pp. 9970–9975. doi: 10.1073/pnas.0803356105.

Du, F., Guan, C. and Jiao, Y. (2018) 'Molecular Mechanisms of Leaf Morphogenesis',

Molecular Plant. Elsevier Ltd, 11(9), pp. 1117–1134. doi: 10.1016/j.molp.2018.06.006.

Emery, J. F. *et al.* (2003) 'Radial Patterning of Arabidopsis Shoots by Class III HD-ZIP and KANADI Genes', *Current Biology*, 13(20), pp. 1768–1774. doi: 10.1016/j.cub.2003.09.035. Gómez-Mena, C. *et al.* (2005) 'Transcriptional program controlled by the floral homeotic gene AGAMOUS during early organogenesis', *Development*, 132(3), pp. 429–438. doi: 10.1242/dev.01600.

Ferrandiz, C., et al. (2000). Redundant regulation of meristem identity and plant architecture by FRUITFULL, APETALA1 and CAULIFLOWER. *Development* 127(4) 725-734.

Goto, K. *et al.* (1994) 'Function and regulation of the A r a b i d o p s i s floral homeotic g e n e PISTIL L A T A', pp. 1548–1560.

Guo, S. *et al.* (2015) 'Co-ordination of flower development through epigenetic regulation in two model species: Rice and arabidopsis', *Plant and Cell Physiology*, 56(5), pp. 830–841. doi: 10.1093/pcp/pcv037.

Hashimoto, K. *et al.* (2018) 'Functionally Diversified Members of the MIR165/6 Gene Family Regulate Ovule Morphogenesis in Arabidopsis thaliana', *Plant and Cell Physiology*, 59(5), pp. 1017–1026. doi: 10.1093/pcp/pcy042.

Heijmans, K. *et al.* (2012) 'Redefining C and D in the petunia ABC', *Plant Cell*, 24(6), pp. 2305–2317. doi: 10.1105/tpc.112.097030.

Honma, T. and Goto, K. (2001) 'Complexes of MADS-box proteins are suf ® cient to convert leaves into ¯ oral organs', 409(January), pp. 525–529.

Huijser, P. and Schmid, M. (2011) 'The control of developmental phase transitions in plants', *Development*, 138(19), pp. 4117–4129. doi: 10.1242/dev.063511.

Inoue, H., Nojima, H. and Okayama, H. (1990) 'High efficiency transformation of Escherichia coli with plasmids', *Gene*, 96(1), pp. 23–28. doi: 10.1016/0378-1119(90)90336-P.

Irish, V. (2017) 'The ABC model of floral development', *Current Biology*. Elsevier, 27(17), pp. R887–R890. doi: 10.1016/j.cub.2017.03.045.

Irish, V. F. and Sussex, I. M. (1990) 'Function of the apetala-1 gene during Arabidopsis floral development.', *The Plant cell*, 2(8), pp. 741–753. doi: 10.1105/tpc.2.8.741.

Ito, T. *et al.* (2004) 'The homeotic protein AGAMOUS controls microsporogeniesis by regulation of SPOROCYTELESS', *Nature*, 430(6997), pp. 356–360. doi: 10.1038/nature02733.

Iwakawa, H. *et al.* (2007) 'Expression of the ASYMMETRIC LEAVES2 gene in the adaxial domain of Arabidopsis leaves represses cell proliferation in this domain and is critical for the development of properly expanded leaves', *Plant Journal*, 51(2), pp. 173–184. doi: 10.1111/j.1365-313X.2007.03132.x.

Jack, T., Fox, G. L. and Meyerowltx, E. M. (1994) 'Homedic Gene AETALA3', 76, pp. 703–716.

Jiang, K. and Feldman, L. J. (2005) 'Regulation of root apical meristem development', *Annual Review of Cell and Developmental Biology*, 21, pp. 485–509. doi: 10.1146/annurev.cellbio.21.122303.114753.

Jiao, Y. *et al.* (2011) 'Ancestral polyploidy in seed plants and angiosperms', *Nature*, 473(7345), pp. 97–100. doi: 10.1038/nature09916.

Jofuku, K. D. *et al.* (1994) 'Control of Arabidopsis flower and seed development by the homeotic gene APETALA2', *Plant Cell*, 6(9), pp. 1211–1225. doi: 10.1105/tpc.6.9.1211.

Juarez, M. T. *et al.* (2004) 'microRNA-mediated repression of rolled leaf1 specifies maize leaf polarity', *Nature*, 428(6978), pp. 84–88. doi: 10.1038/nature02363.

Kaplan, D.R., (2001). Fundamental concepts of leaf morphology and morphogenesis: a contribution to the interpretation of molecular genetic mutants. *International Journal of Plant Sciences*, *162*(3), pp.465-474.

Kaufmann, K. *et al.* (2010) 'Orchestration of floral initiation by APETALA1', *Science*, 328(5974), pp. 85–89. doi: 10.1126/science.1185244.

Kaufmann, K., Melzer, R. and Theißen, G. (2005) 'MIKC-type MADS-domain proteins: Structural modularity, protein interactions and network evolution in land plants', *Gene*, 347(2 SPEC. ISS.), pp. 183–198. doi: 10.1016/j.gene.2004.12.014.

Kelley, D. R., Skinner, D. J. and Gasser, C. S. (2009). Roles of polarity determinants in ovule development. *Plant J.* 57, 1054-1064.

Kerstetter, R.A., Bollman, K., Taylor, R.A., Bomblies, K. and Poethig, R.S., (2001). KANADI regulates organ polarity in Arabidopsis. *Nature*, *411*(6838), pp.706-709.

Kidner, C. A. and Timmermans, M. C. P. (2010) 'Signaling sides. Adaxial-abaxial patterning in leaves', *Current Topics in Developmental Biology*, 91(C), pp. 141–168. doi: 10.1016/S0070-2153(10)91005-3.

Kinoshita, A. and Richter, R. (2020) 'Genetic and molecular basis of floral induction in Arabidopsis thaliana', *Journal of Experimental Botany*, 71(9), pp. 2490–2504. doi: 10.1093/jxb/eraa057.

Kramer, M. F. (2011) 'Stem-loop RT-qPCR for miRNAs', *Current Protocols in Molecular Biology*, (SUPPL. 95), pp. 1–15. doi: 10.1002/0471142727.mb1510s95.

Krizek, B. A. and Fletcher, J. C. (2005) 'Molecular mechanisms of flower development: An armchair guide', *Nature Reviews Genetics*, 6(9), pp. 688–698. doi: 10.1038/nrg1675.

Krogan, N. T., Hogan, K. and Long, J. A. (2012) 'APETALA2 negatively regulates multiple floral organ identity genes in Arabidopsis by recruiting the co-repressor TOPLESS and the histone deacetylase HDA19', *Development*, 139(22), pp. 4180–4190. doi: 10.1242/dev.085407.

Lee, J. Y. *et al.* (2005) 'Activation of CRABS CLAW in the nectaries and carpels of arabidopsis', *Plant Cell*, 17(1), pp. 25–36. doi: 10.1105/tpc.104.026666.

Lee, Z. H. *et al.* (2019) 'CRABS CLAW and SUPERMAN Coordinate Hormone-, Stress-, and Metabolic-Related Gene Expression During Arabidopsis Stamen Development', *Frontiers in Ecology and Evolution*, 7. doi: 10.3389/fevo.2019.00437.

Li, H. T. *et al.* (2019) 'Origin of angiosperms and the puzzle of the Jurassic gap', *Nature Plants*. Springer US, 5(5), pp. 461–470. doi: 10.1038/s41477-019-0421-0.

Li, X. *et al.* (2019) 'MicroRNA166 monitors SPOROCYTELESS/NOZZLE for building of the anther internal boundary', *Plant Physiology*, 181(1), pp. 208–220. doi: 10.1104/pp.19.00336.

Liu, C., Thong, Z. and Yu, H. (2009) 'Coming into bloom: The specification of floral meristems', *Development*, 136(20), pp. 3379–3391. doi: 10.1242/dev.033076.

Liu, H. *et al.* (2018) 'Small but powerful: function of microRNAs in plant development', *Plant Cell Reports*. Springer Berlin Heidelberg, 37(3), pp. 515–528. doi: 10.1007/s00299-017-2246-5.

Liu, T. *et al.* (2012) 'Of blades and branches: Understanding and expanding the arabidopsis ad/abaxial regulatory network through target gene identification', *Cold Spring Harbor Symposia on Quantitative Biology*, 77(C), pp. 31–45. doi: 10.1101/sqb.2013.77.014480.

Liu, X. *et al.* (2009) 'The SPOROCYTELESS/NOZZLE gene is involved in controlling stamen identity in Arabidopsis', *Plant Physiology*, 151(3), pp. 1401–1411. doi: 10.1104/pp.109.145896.

Mandel, M. A., Gustafson-Brown, C., Savidge, B. & Yanofsky, M. F. (1992) Molecular characterization of the Arabidopsis floral homeotic gene APETALA1. *Nature* 360, 273±277

Manuela, D. and Xu, M. (2020) 'Patterning a Leaf by Establishing Polarities', *Frontiers in Plant Science*, 11(October), pp. 1–15. doi: 10.3389/fpls.2020.568730.

Mcconnell, J. R. *et al.* (2001) 'Role of PHABULOSA and PHAVOLUTA in determining radial patterning in shoots._McConnell et al', 411(June), pp. 709–713.

Merelo, P. *et al.* (2013) 'Genome-Wide Identification of KANADI1 Target Genes', *PLoS ONE*, 8(10), pp. 1–14. doi: 10.1371/journal.pone.0077341.

Merelo, P. *et al.* (2016) 'Regulation of MIR165/166 by class II and class III homeodomain leucine zipper proteins establishes leaf polarity', *Proceedings of the National Academy of Sciences of the United States of America*, 113(42), pp. 11973–11978. doi: 10.1073/pnas.1516110113.

Mizukami, Y. and Ma, H. (1992) Ectopic Expression of the Floral Homeotic Gene AGAMOUS in Transgenic Arabidopsis Plants Alters Floral Organ Identity. *Cell*, 71, 119-131.

Nakata, M. and Okada, K. (2013) 'The leaf adaxial-abaxial boundary and lamina growth', *Plants*, 2(2), pp. 174–202. doi: 10.3390/plants2020174.

Nakaya, M. *et al.* (2002) 'Brassinosteroids control the proliferation of leaf cells of Arabidopsis thaliana', *Plant and Cell Physiology*, 43(2), pp. 239–244. doi: 10.1093/pcp/pcf024.

Ó'Maoiléidigh, D. S. *et al.* (2018) 'Floral homeotic proteins modulate the genetic program for leaf development to suppress trichome formation in flowers', *Development (Cambridge)*, 145(3). doi: 10.1242/dev.157784.

O'Maoileidigh, D. S. *et al.* (2013) 'Control of Reproductive Floral Organ Identity Specification in Arabidopsis by the C Function Regulator AGAMOUS', *The Plant Cell*, 25(7), pp. 2482–2503. doi: 10.1105/tpc.113.113209.

Ó'Maoiléidigh, D. S., Graciet, E. and Wellmer, F. (2014) 'Gene networks controlling Arabidopsis thaliana flower development', *New Phytologist*, 201(1), pp. 16–30. doi: 10.1111/nph.12444.

Okamuro, J K *et al.* (1997) 'Photo and hormonal control of meristem identity in the

Arabidopsis flower mutants apetala2 and apetala1.', *The Plant cell*, 9(1), pp. 37–47. doi: 10.1105/tpc.9.1.37.

Okamuro, Jack K. *et al.* (1997) 'The AP2 domain of APETALA2 defines a large new family of DNA binding proteins in Arabidopsis', *Proceedings of the National Academy of Sciences of the United States of America*, 94(13), pp. 7076–7081. doi: 10.1073/pnas.94.13.7076.

Okuma, N. *et al.* (2020) 'MIR2111-5 locus and shoot-accumulated mature miR2111 systemically enhance nodulation depending on HAR1 in Lotus japonicus', *Nature Communications*. Springer US, 11(1), pp. 1–13. doi: 10.1038/s41467-020-19037-9.

Pajoro, A., Madrigal, P., *et al.* (2014) 'Dynamics of chromatin accessibility and gene regulation by MADS-domain transcription factors in flower development', *Genome Biology*, 15(3). doi: 10.1186/gb-2014-15-3-r41.

Pajoro, A., Biewers, S., *et al.* (2014) 'The (r)evolution of gene regulatory networks controlling Arabidopsis plant reproduction: A two-decade history', *Journal of Experimental Botany*, 65(17), pp. 4731–4745. doi: 10.1093/jxb/eru233.

Pařenicová, L. *et al.* (2003) 'Molecular and phylogenetic analyses of the complete MADS-Box transcription factor family in Arabidopsis: New openings to the MADS world', *Plant Cell*, 15(7), pp. 1538–1551. doi: 10.1105/tpc.011544.

Pattanaik, S. *et al.* (2014) 'An overview of the gene regulatory network controlling trichome development in the model plant , Arabidopsis', 5(June), pp. 1–8. doi: 10.3389/fpls.2014.00259.

Payne T, Johnson SD, Koltunow AM. (2004). KNUCKLES (KNU) encodes a C2H2 zinc-finger protein that regulates development of basal pattern elements of the Arabidopsis gynoecium. *Development* 131: 3737–3749.

Pekker, I., Alvarez, J. P. and Eshed, Y. (2005) 'Auxin response factors mediate Arabidopsis organ asymmetry via modulation of KANADI activity', *Plant Cell*, 17(11), pp. 2899–2910. doi: 10.1105/tpc.105.034876.

Pelaz, S. *et al.* (2001) 'Conversion of leaves into petals in Arabidopsis', *Current Biology*, 11(3), pp. 182–184. doi: 10.1016/S0960-9822(01)00024-0.

Ramírez-Barahona, S., Sauquet, H. and Magallón, S. (2020) 'The delayed and geographically heterogeneous diversification of flowering plant families', *Nature Ecology and Evolution*, 4(9), pp. 1232–1238. doi: 10.1038/s41559-020-1241-3.

Rodríguez, A. *et al.* (2020) 'Comparison of procedures for RNA-extraction from peripheral blood mononuclear cells', *PLoS ONE*, 15(2), pp. 1–17. doi: 10.1371/journal.pone.0229423.

Ryan, P. T. *et al.* (2015) 'Patterns of gene expression during Arabidopsis flower development from the time of initiation to maturation', *BMC Genomics*, 16(1), pp. 1–12. doi: 10.1186/s12864-015-1699-6.

Schroeder, A. *et al.* (2006) 'The RIN: An RNA integrity number for assigning integrity values to RNA measurements', *BMC Molecular Biology*, 7, pp. 1–14. doi: 10.1186/1471-2199-7-3.

Schwarz-Sommer, Z. *et al.* (1990) 'Genetic Control of Flower Development by Homeotic Genes in Antirrhinum majus.', *Science (New York, N.Y.)*, 250(4983), pp. 931–6. doi: 10.1126/science.250.4983.931.

Shang, E., Ito, T. and Sun, B. (2019) 'Control of floral stem cell activity in Arabidopsis', *Plant Signaling and Behavior*. doi: 10.1080/15592324.2019.1659706.

Sharma A, et al. (2002). miRNPs: a novel class of ribonucleoproteins containing numerous microRNAs. *Genes Dev* 16: 720–8

Siegfried, K. R. *et al.* (1999) 'Members of the YABBY gene family specify abaxial cell fate in Arabidopsis', *Development*, 126(18), pp. 4117–4128.

Skopelitis, D. S. *et al.* (2017) 'Boundary Formation through a Direct Threshold-Based Readout of Mobile Small RNA Gradients', *Developmental Cell*. Elsevier Inc., 43(3), pp. 265-273.e6. doi: 10.1016/j.devcel.2017.10.003.

Smyth, D. R. (1990) 'Early Flower Development in Arabidopsis', *the Plant Cell Online*, 2(8), pp. 755–767. doi: 10.1105/tpc.2.8.755.

Snow, R. and Snow, M. (1954) 'Experiments on the cause of dorsiventrality in leaves', *Nature*, 174(4425), pp. 352–353. doi: 10.1038/174352a0.

Soltis, P. S., Folk, R. A. and Soltis, D. E. (2019) 'Darwin review: angiosperm phylogeny and evolutionary radiations', *Proceedings of the Royal Society B: Biological Sciences*, 286(1899), p. 20190099. doi: 10.1098/rspb.2019.0099.

Sun, B. *et al.* (2009) 'A timing mechanism for stem cell maintenance and differentiation in the Arabidopsis floral meristem', *Genes and Development*, 23(15), pp. 1791–1804. doi: 10.1101/gad.1800409.

Sussex, I.M., (1951). Experiments on the cause of dorsiventrality in leaves. *Nature*, *167*(4251), pp.651-652

Srikanth, A. and Schmid, M. (2011). Regulation of flowering time: all roads lead to Rome. Cell. Mol. Life Sci. 68, 2013-2037

Theißen, G. & Saedler, H. (2001) Floral quartets. *Nature* 409, 469–471

Theissen, G. and Melzer, R. (2007) 'Molecular mechanisms underlying origin and diversification of the angiosperm flower', *Annals of Botany*, 100(3), pp. 603–619. doi: 10.1093/aob/mcm143.

Theißen, G., Melzer, R. and Ruümpler, F. (2016) 'MADS-domain transcription factors and the floral quartet model of flower development: Linking plant development and evolution', *Development (Cambridge)*, 143(18), pp. 3259–3271. doi: 10.1242/dev.134080.

Thomson, B. (2017) 'Analysis of stage-specific gene perturbations and characterisation of two novel F-box genes during flower development in Arabidopsis thaliana' *Trinity College Dublin.School of Genetics & Microbiology*

Thomson, B. and Wellmer, F. (2019) *Molecular regulation of flower development*. 1st edn,

Current Topics in Developmental Biology. 1st edn. Elsevier Inc. doi: 10.1016/bs.ctdb.2018.11.007.

Toni, L. S. *et al.* (2018) 'Optimization of phenol-chloroform RNA extraction', *MethodsX*. Elsevier B.V., 5, pp. 599–608. doi: 10.1016/j.mex.2018.05.011.

Uhrig, J. F. and Hülskamp, M. (2010) 'Trichome Development in Arabidopsis BT - Plant Mitochondria', *Plant Mitochondria*, 655(Chapter 6), pp. 77–88. doi: 10.1007/978-1-60761-765-5.

von Goethe, J. W. (1790). Versuch die Metamorphose der Pflanzen zu erklä ren. Gotha, Germany: Ettinger.

Wagner, D. (2017) 'Key developmental transitions during flower morphogenesis and their regulation', *Current Opinion in Genetics and Development*. Elsevier Ltd, 45, pp. 44–50. doi: 10.1016/j.gde.2017.01.018.

Waheed, S. and Zeng, L. (2020) 'The critical role of miRNAs in regulation of flowering time and flower development', *Genes*, 11(3), pp. 1–24. doi: 10.3390/genes11030319.

Wellmer, F. *et al.* (2004) 'Genome-wide analysis of spatial gene expression in arabidopsis flowers', *Plant Cell*, 16(5), pp. 1314–1326. doi: 10.1105/tpc.021741.

Wellmer, F. *et al.* (2006) 'Genome-wide analysis of gene expression during early Arabidopsis flower development', *PLoS Genetics*, 2(7), pp. 1012–1024. doi: 10.1371/journal.pgen.0020117.

Wollmann, H. *et al.* (2010) 'On reconciling the interactions between APETALA2, miR172 and AGAMOUS with the ABC model of flower development', *Development*, 137(21), pp. 3633–3642. doi: 10.1242/dev.036673.

Wu, R. *et al.* (2007) 'Real-Time PCR Quantification of Plant miRNAs Using Universal ProbeLibrary Technology', *Biochemica*, (2), pp. 12–15. Available at: https://www.roche-applied-science.com/wcsstore/RASCatalogAssetStore/Articles/BIOCHEMICA_2_07_p12-15.pdf.

Wuest, S. E. *et al.* (2012) 'Molecular basis for the specification of floral organs by APETALA3 and PISTILLATA', *Proceedings of the National Academy of Sciences of the United States of America*, 109(33), pp. 13452–13457. doi: 10.1073/pnas.1207075109.

Xie, Y. *et al.* (2015) 'Meta-analysis of arabidopsis KANADI1 direct target genes identifies a basic growth-promoting module acting upstream of hormonal signaling pathways', *Plant Physiology*, 169(2), pp. 1240–1253. doi: 10.1104/pp.15.00764.

Xie, Z. *et al.* (2005) 'Expression of Arabidopsis MIRNA genes', *Plant Physiology*, 138(4), pp. 2145–2154. doi: 10.1104/pp.105.062943.

Xu, M. *et al.* (2016) 'Developmental Functions of miR156-Regulated SQUAMOSA PROMOTER BINDING PROTEIN-LIKE (SPL) Genes in Arabidopsis thaliana', *PLoS Genetics*, 12(8), pp. 1–29. doi: 10.1371/journal.pgen.1006263.

Xu, Y. *et al.* (2019) 'When to stop: An update on molecular mechanisms of floral meristem termination', *Journal of Experimental Botany*, 70(6), pp. 1711–1718. doi: 10.1093/jxb/erz048.

Yamada, T. *et al.* (2016) 'CORONA, PHABULOSA AND PHAVOLUTA collaborate with BELL1 to confine WUSCHEL expression to the nucellus in Arabidopsis ovules', *Development (Cambridge)*, 143(3), pp. 422–426. doi: 10.1242/dev.129833.

Yamaguchi, T., Nukazuka, A. and Tsukaya, H., (2012). Leaf adaxial–abaxial polarity specification and lamina outgrowth: evolution and development. *Plant and Cell Physiology*, *53*(7), pp.1180-1194.

Yang, T. *et al.* (2019) 'The interaction between miR160 and miR165/166 in the control of leaf development and drought tolerance in Arabidopsis', *Scientific Reports*, 9(1), p. 2832. doi: 10.1038/s41598-019-39397-7.

Yanofsky, M. F. *et al.* (1990) 'The protein encoded by the Arabidopsis homeotic gene agamous resembles transcription factors', *Nature*, 346(6279), pp. 35–39. doi: 10.1038/346035a0.